

We are IntechOpen, the world's leading publisher of Open Access books Built by scientists, for scientists

6,900

Open access books available

186,000

International authors and editors

200M

Downloads

Our authors are among the

154

Countries delivered to

TOP 1%

most cited scientists

12.2%

Contributors from top 500 universities



WEB OF SCIENCE™

Selection of our books indexed in the Book Citation Index
in Web of Science™ Core Collection (BKCI)

Interested in publishing with us?
Contact book.department@intechopen.com

Numbers displayed above are based on latest data collected.
For more information visit www.intechopen.com



Treating of Waste Water Applying Bubble Flotation

Ramiro Escudero, Francisco J. Tavera and Eunice Espinoza

Additional information is available at the end of the chapter

<http://dx.doi.org/10.5772/54227>

1. Introduction

Recently, it might be exaggerated the impact of man activities as the solely cause of the tremendous changes in the global climate resulting from its activity effects on the environment nature; it has been suggested that it has started a new geological era, the “antroposoic age;” however, there are some clues, together with man influence in climate changes, that sun activity has a determining effect on the subject. Nevertheless, from the beginning of man species presence in the geological record it is observed an interaction of these species with the surroundings that increases with their degree of social and technological development.

The association between man and its environment presents a continuous growth because the development of its intellect and the complex nature of its thought; these features allowed man to adapt to a variety of geographical situations, spreading towards the entire planet, building technologies as a result of its social development needs.

In the historic record of civilization, in modern times, between the second half of the 1700’s and the middle of the 1800’s, there is an exponential increase in natural resources exploitation because the advance in the scientific knowledge and the technological development. The expansion trend of these features, the science and technology, has been maintained with no interruption, as well as their effect on the surroundings producing a deleterious consequence on the environs quality.

It is well understood that the equilibrium in the planet nature is very sensitive to man activities, therefore, it is necessary to intensify the carefulness to preserve the ecosystem quality in order to prevent catastrophic environmental disasters.

A critic facet of natural environment is related to water pollution. Depletion of fresh water reserves makes it important to propose effective technologies to clean and recover water

from polluted water network. Therefore, advances in possible water treating improvements are issued in this chapter.

2. Treating of waste water applying bubble flotation

From the time when natural resources started to be exploited in a massive way, water is used as a vehicle to transport and process materials. Water is the most important solvent in nature, and the contact of water with a variety of substances makes it the origin of water pollution through the formation of dissolved solutes solutions which decrease the quality of the liquid.

Water is often encountered with high concentration of pollutants that could be in solution or dispersed as insoluble phases frequently forming emulsions and colloids. Among pollutants encountered in fresh water are heavy metals and organics. These materials regularly are difficult to process because of the enormous amounts of water that is produced by urban and industrial activities; therefore, the ideal process to clean polluted water should be operating in a continuous way to minimise fixed and operating costs.

2.1. Lead carbonate colloid in residual water: continuous ion flotation

The ion flotation term was first introduced by Sebba [1], defined it as a technique used to collect a material which is in solution in an aqueous phase, and it may be even in a colloid structure. By adding modifiers of the chemical conditions of the aqueous media, and with the addition of a collector reagent, adequately electrically charged, the dissolved substance, or the colloid, is transformed in a product with hydrophobic sites which promotes its adsorption on the liquid/vapour "surface" of a gas bubble and, therefore, to float in the aqueous media up to its surface producing a foam that contains a concentrate of the original substance which can be collected.

By looking into the previous statement, it can be thought that there is a concentration relationship between the amount of dissolved substance and the required amount of collector reagent to create hydrophobic sites. Therefore, ion flotation technique is restricted to treat dilute aqueous solutions of such ion or colloid material, otherwise, the required amount of collector reagent may exceed the micelle critical concentration and the desired process would not be attained.

The goal idea in the application of ion or colloid flotation techniques may be to treat residual industrial or urban water, which means that it has to deal with enormous amounts of water and, therefore, a continuous process should be available to separate the solute impurity.

In the case of flotation as applied to mineral particles, it requires the gas bubbles to be large enough to produce a solid-bubble aggregate with a lower relative density than the mineral pulp density which is processed and, in this case, bubble shear must be controlled to avoid the detachment of solids from the bubble.

However, in ion flotation the material to be separated from the liquid presents a similar density as that of the liquid bulk, and the inertia of this material in front of the moving gas

bubbles is such that it can be easily drawn by the liquid that flows surrounding the bubble. Consequently, it may be expected that the contact between the hydrophobic material and the gas bubble will be likely to occur by decreasing bubble size; in addition, when the formation of small bubbles takes place, it creates a larger gas surface area which improves the flotation process [2, 3].

Most of the experimental work reported on ion flotation has been carried out in flotation columns may be under the influence of a better performance of column flotation in mineral processing. In spite of this, the ascending bubbles in a liquid column produce axial mixing and turbulences that prevent an effective contact among the floatable material and the gas bubble.

At the present time, the ion flotation technique has not reached any commercial appliance; nevertheless, there are good expectations for different engineering applications. A possibility in commercial scale might be the treating of aqueous media containing heavy metals.

The presence of heavy metals in residual water is commonly observed as a product of mining and metallurgical works; if these waters are discharged directly this will cause a major environmental problem; therefore, it is necessary to treat these waters to remove impurities to acceptable levels to avoid any damage to the environment. However, still today, in some locations, the exigencies to keep a close control on the application of environmental regulations are poor and serious pollution problems exist [4].

To correct the problem, engineering work must be dedicated to produce a realistic procedure for its application in large scale as it is required in mining and metallurgical locations.

It has been proposed and validated in laboratory, and pilot plant tests, the use of froth flotation to treat lead polluted water in a continuous scheme operation. In that case, lead is present in the aqueous phase as a lead colloidal carbonate, with a lead concentration of 20 ppm. A series of sparged flotation cells are used to perform the separation of the lead specie [5]; Figure 1 shows a representation of the series of flotation cells.

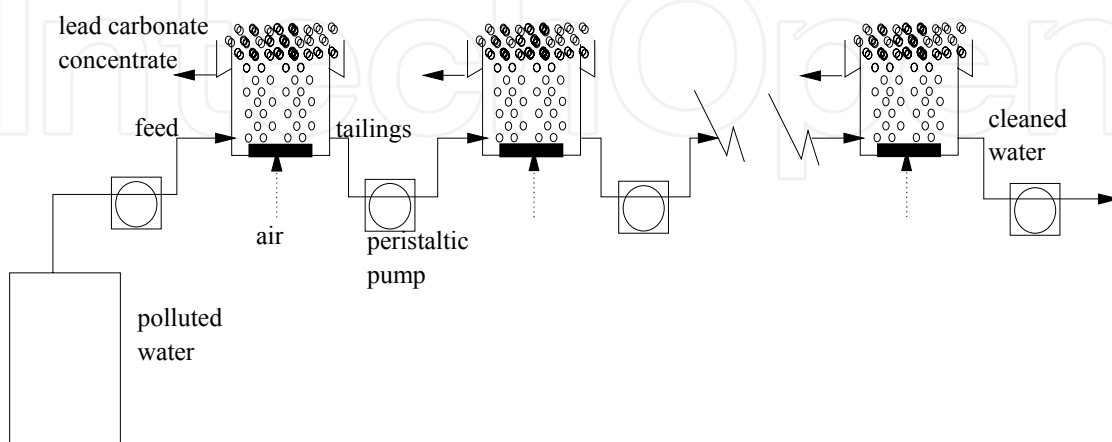


Figure 1. Illustration of a series of sparged flotation cells where porous gas spargers are installed to inject-disperse air in the form of small gas bubbles (< 1.5 mm).

In this flotation process, the water containing the lead colloidal carbonate is adequately conditioned by the addition of chemical reagent to fix an adequate pH to make possible to complex the lead specie with a suitable flotation reagent. Gas hold-up was measured below the froth region in the flotation cells by pressure measurements [3, 6], and locally at different points measuring electrical conductivity [7]; these measurements were related to the efficiency of producing large gas surface areas to perform the collection process of hydrophobic species.

In designing the chemical characteristics of the process, for example the pH of the aqueous phase, and the type of collector reagent, lead carbonate particles were separated and analysed in their Zeta potential (ζ) behaviour. Figure 2 shows the ζ performance of the lead carbonate.

The polluted water presented a pH of 7.4, therefore a cationic collector was used to produce a hydrophobic behaviour to the lead carbonate particles. The series of flotation cells were operated until the steady state conditions were achieved. At this point an apparent residence time was estimated ($\tau = [h_{cz}/J_l] \times [1 - \varepsilon_g]$; where h_{cz} is the collection zone height measured from the bottom to the froth interface, J_l is the superficial liquid velocity, and ε_g is the gas hold-up); as a first approximation this representation of residence time may be used to express the nature of mixing in the series of flotation cells.

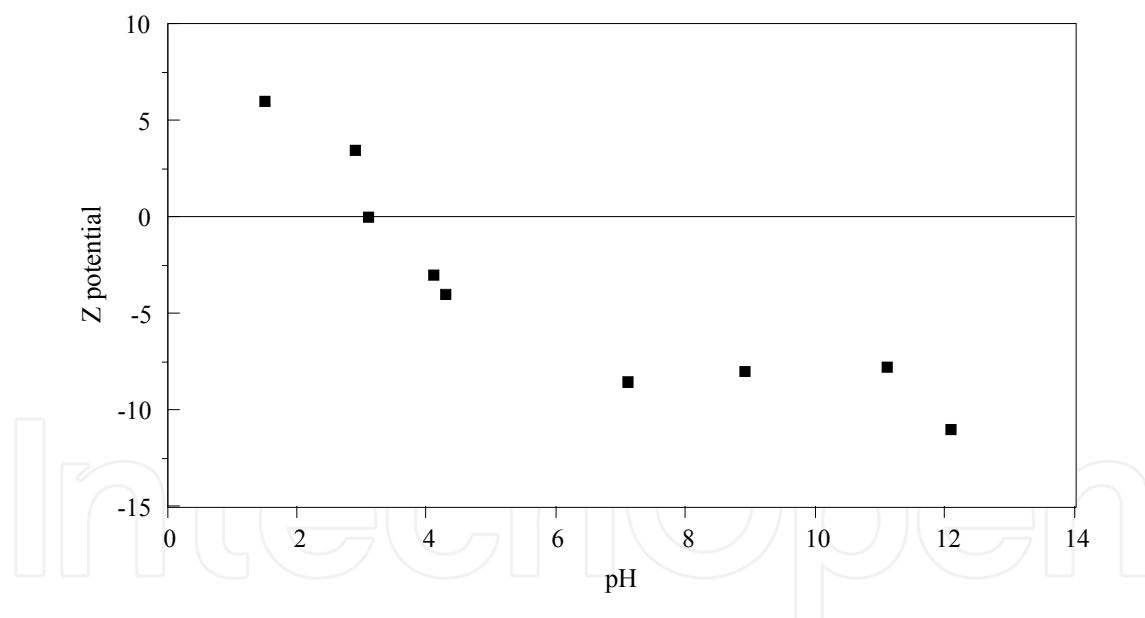


Figure 2. Measurements on the behaviour of Zeta potential (ζ) lead carbonate; measurements through the pH range between 1.4 and 12.

The different streams (concentrate, tailings, and feed) were sampled to analyse their concentration of lead, and to determine the recovery of this material through the separation process. The recovery of lead may be related to the characteristics of the process in terms of the variables ε_g , bubble size, the superficial bubble surface flux, and the kinetics of the process.

During the operation of the series of flotation cells, gas hold-up was monitored continuously in each flotation cell using measurements of pressure and electrical conductivity [6, 9].

Figure 3 presents the lead recovery in concentrate as a function of gas hold-up change in the first flotation cell.

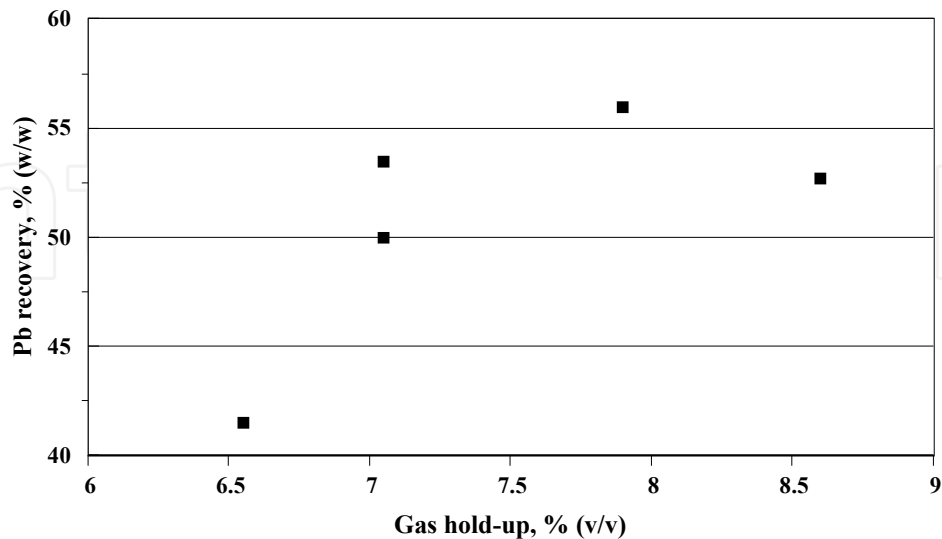


Figure 3. Typical graphic of experimental results on the flotation of lead represented as the lead recovery % and the corresponding gas hold-up.

The lead reported to the concentrate shows that its recovery increases as the amount of gas in the gas-water dispersion rises, as a result of the increase in the availability of bubble surface area to perform the collection process of hydrophobic species. The flotation of the lead specie presents a steady increase with increasing until the gas hold-up reaches 7.7% (v/v) above which there is a sudden reduction on that operation variable due to the formation of excessive turbulence produced by a considerable flow of gas in the cell.

Nevertheless, the magnitude of gas hold-up is related to bubble size, beside to the amount of gas which is fed into the flotation system. This may imply that the production of large gas hold-ups is related to formation of small gas bubbles. In this way, the recovery of lead from the aqueous media should be upgraded with the bubble size reduction. This effect is shown in Figure 4.

The bubble dimension was estimated by two methods: first a direct method using image analysis [10]; and the indirect method of drift flux analysis [3].

The experimental practice indicates that the decrease in the diameter of gas bubbles produces larger bubble surface area which “flows” through the flotation system collecting the hydrophobic species as they have a collision.

Production of large bubbles presents a hydrodynamic effect in the collection process, in addition to a smaller bubble surface area, which decreases the collection of lead carbonate colloid by minimizing the possible collision between the gas bubble and the hydrophobic lead carbonate surface. The contribution of these two effects of the bubble surface area is shown in fig. 4.

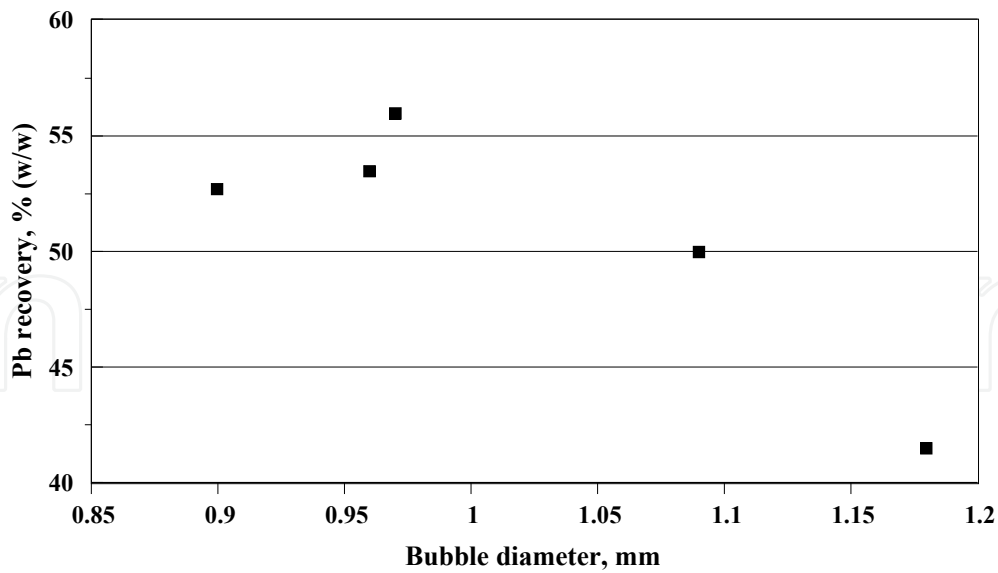


Figure 4. Effect of the bubble size on the separation of lead from the aqueous media.

In terms of the bubble surface area, the concept of “superficial bubble surface flux,” S_b , has been suggested as a controlling ultimate flotation variable. S_b contains the chemical, hydrodynamics, and mechanical characteristics of the flotation system; S_b can be thought as the amount of bubble surfaces that flow through a unit of a cross sectional area normal to the bubbles motion, by unit of time, therefore with units of time^{-1} ; therefore from geometry considerations, $S_b = 6 (J_g/d_b)$, where J_g is the superficial gas velocity, and d_b is the bubble diameter [11]. It has been demonstrated that S_b is directly related to the flotation – separation kinetics [12]. Figure 5 shows the relationship between the recovery of floated lead and S_b .

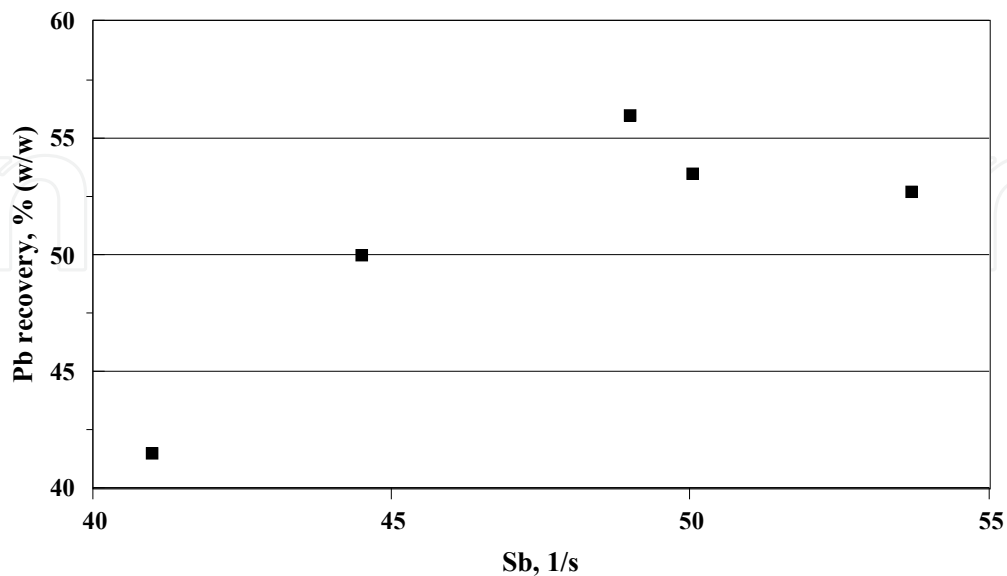


Figure 5. Relationship between the separation of lead carbonate from the aqueous phase by flotation, and the superficial bubble surface flux.

It can be noticed that the separation of lead from the water increases as the available bubble surface rises. Nevertheless, there is a maximum value of the lead recovery which corresponds to a given S_b value.

Above that S_b value, the relationship between P_b recovery and S_b changes due to an increase of mixing and circulation in the flotation system. This information indicates that the flotation of the lead colloid carbonate is very sensitive to the bubble size change, and therefore, to the superficial gas velocity and the superficial liquid velocity.

The behaviour of the flotation cells follow a model of the perfect mixer, therefore, flotation constant rate may be expressed as $\kappa = R/[\tau (1 - R)]$, where R is the lead recovery expressed as the weight fraction.[13]

The apparent rate constant for the lead colloid carbonate flotation is presented in Figure 6 as a function of the gas hold-up in the collection zone.

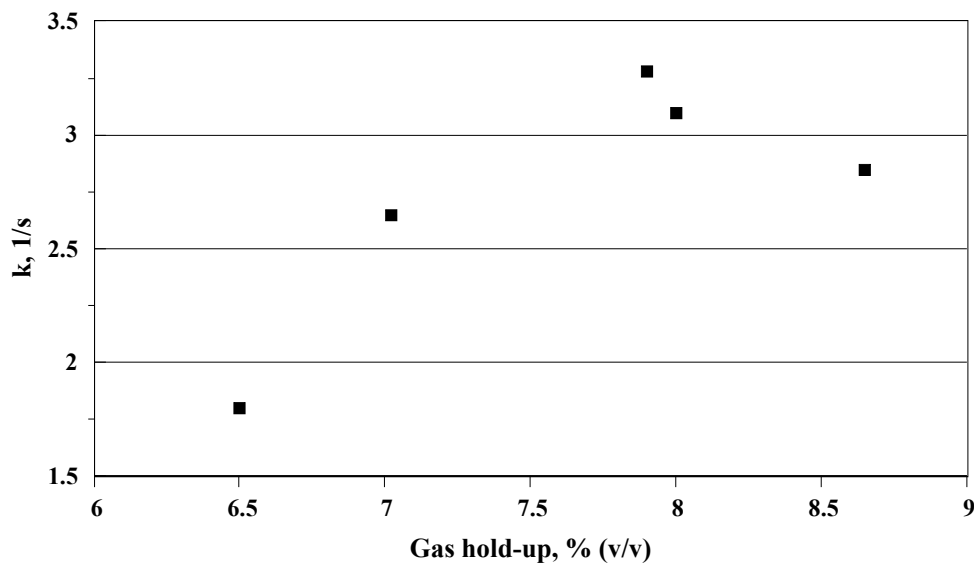


Figure 6. Behaviour of the apparent rate constant, as a function of the change on gas hold-up in the flotation of lead colloid carbonate.

It is observed that the flotation rate constant follows a linear relationship with respect to the change in the gas hold-up if the last is kept below 8%. Above this gas hold-up value the correlation between the flotation kinetics and the gas hold-up changes. This information suggests that the lead colloid carbonate flotation rate is strongly dependent from the hydrodynamic conditions of the system.

The previous statement indicates that the flotation rate constant must be related to the bubble size. Figure 7 presents the relationship between the flotation rate constant for the separation of the lead colloid carbonate, and the estimated bubble size.

This information describes that when the bubble size is between 0.97 mm and 1.2 mm presents a linear correlation with the apparent flotation rate constant. In this range of bubble size it can be seen that the kinetics of the flotation process is favoured with the decrease in

the bubble diameter. But with the increase in bubble size above 1.2 mm the possibility to have a collision between the lead colloid carbonate and the bubble decreases, because the hydrodynamics of the bubble that moves faster in the liquid bulk.

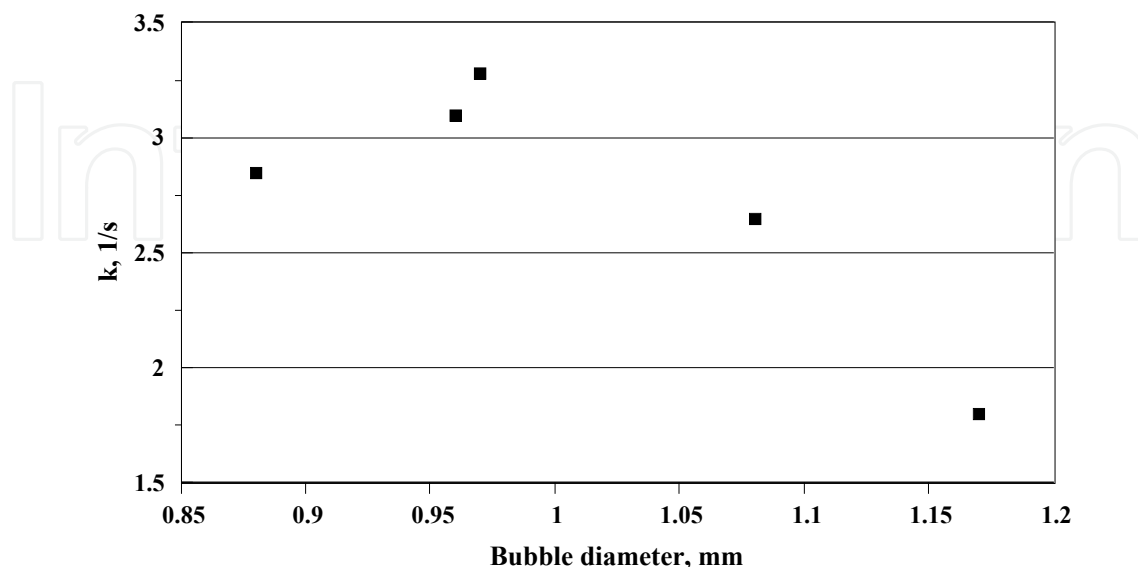


Figure 7. Relationship between the apparent rate constant and bubble size in the lead carbonate colloid separation.

When bubble size is smaller than 0.97 mm the linear trend between the apparent rate constant and bubble size is distorted because the effect of axial mixing. This axial mixing is formed by radial differences of gas distribution, becoming more evident as the gas hold-up increases.

In the series of flotation cells, the superficial gas velocity was maintained at 0.8 cm/s in each flotation cell, and the superficial liquid velocity was kept at 0.19 cm/s.

The lead carbonate colloid cumulative recovery, in the series of flotation cells, was estimated from the mass assaying in each cell.

Figure 8 represents the cumulative recovery of lead as a function of the number of flotation cells in the series of five flotation cells.

It is observed in fig. 8 that the cumulative recovery of lead through the series of 5 flotation cells is 93% (w/w). The total residence time of water in the flotation circuit is 13 minutes. This water processing time gives the impression that is short, as compared with the reported processing times in laboratory flotation columns testing (between 30 to several hundreds of minutes) [2].

This information indicates that the flotation cells instrumented with porous gas bubble generators can produce satisfactory bubble sizes to perform colloid flotation; it seems that differences in bubble size distribution are low enough to reduce axial mixing as compared with the natural circulation presented in flotation columns [13]. In this case lead content in water is reduced from 20 ppm to about 1 ppm.

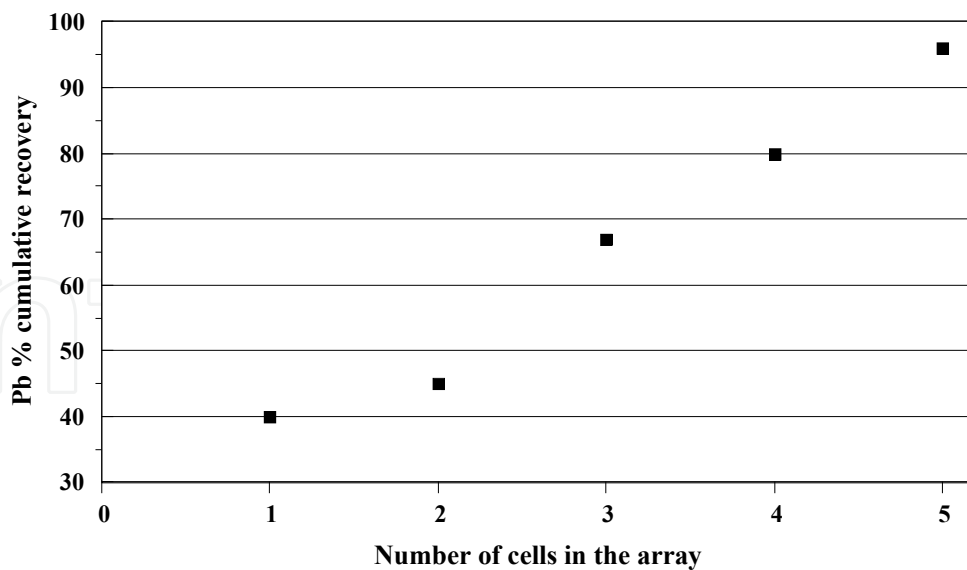


Figure 8. Cumulative recovery of floated lead as a function of the number of flotation cells series.

2.2. Water de-oiling using column flotation

Insoluble organic compounds in water are often encountered as pollutants, particularly in locations near urban centres or in regions associated with industrial and agricultural activities. Among these pollutants oily materials are frequently present in discharged water and should be removed from the aqueous phase before its emission.

In the production of food products such as vegetable cooking oil, residual water contains vestiges of oil, soap, and suspended solid particles from the processed oily seeds. Commonly, pollutants and water forms stable emulsions where the different phases are not easily coagulated and separated by differences of their densities.

In treating such emulsion products, different several approaches are used to eliminate the problem. Bacterial processing is often used to decompose the organic materials generating some non pollutant products; in these biological processes special care must be taken in providing adequate aeration and pH conditions of the polluted water in treating reactors where materials must stay for a while to be processed by living microorganisms. Some other techniques include water evaporation – condensation, but the cost tends to be high by the energy required to evaporate the water from the emulsion.

In searching for a short residence time process that allows to treat continuously large amounts of water, it was studied the possible separation of the organics content in water using flotation techniques.

The use of flotation columns is reported as a possible solution to the problem [14], which implies a simple operation at a very low cost [3].

It was processed industrial residual water from a vegetable oil producer. The polluted water contained 40% v/v of organics consisted of residual oil, soap and solid particles, originated from the oil extraction and refining operations, in processing oily vegetable seeds.

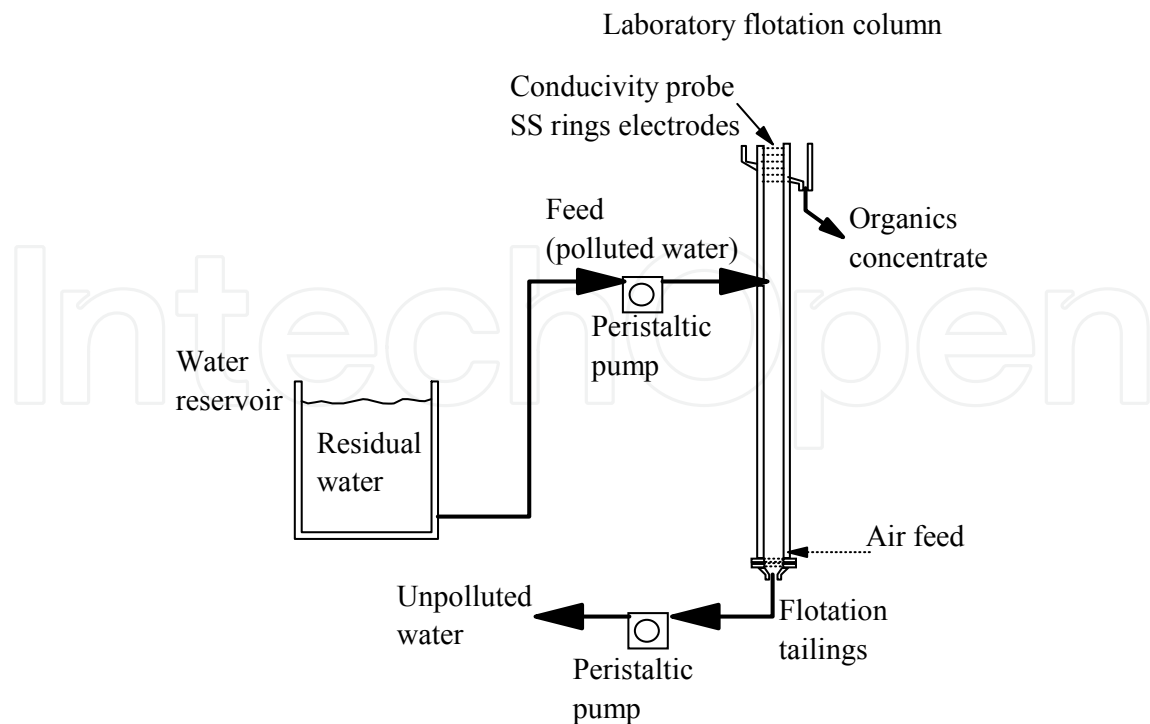


Figure 9. Representation of the laboratory flotation column assembly used to remove organics (oil, soap, solids) from water by froth flotation.

The flotation column was 0.1 m in diameter and 4 m height, and was fully instrumented to be operated automatically. The raw residual polluted water derived from the outlet water circuit at the industrial plant was placed in a 3 m³ reservoir from where the flotation column water feed was continuously taken. The flotation column feed and tailings flow rates were controlled to their desired values using automated peristaltic pumps. The gas hold-up was estimated by measurements of hydrostatic pressure at two heights in the column by means of electronic pressure transmitters. The froth depth was maintained at 10 cm (! 5 cm) from the column lip by varying the feed pump operation to rise or drop the froth zone-collection zone interface; the position of the froth level was monitored using an electrical conductivity probe which consisted of 6 steel ring electrodes placed flushed at the internal wall of the upper part of the column, within 5 cm separately.

The superficial liquid velocity in the column was controlled by controlling to desired values the liquid flow rate controlling the tailings pump. The air was feed into the flotation column through a porous gas sparger made with filter cloth. The air flow rate in the column was measured and controlled in desired values by means of a mass air flow rate controller. The bubble diameter was estimated using drift flux analysis and validated against direct photographic image analysis. The flotation column was made of transparent acrylic, in such manner is possible to visually observe the presence of bubble coalescence, circulation and mixing, under different operating conditions.

In the first approximation a single laboratory flotation column was operated varying the superficial gas velocity under predetermined superficial liquid velocity conditions. The flotation measurements indicate that the flotation of organics is highly affected by the

relative velocities between the liquid flow rate and the gas flow rate. The performance in the flotation column is reported to increase circulation and mixing as the liquid and gas flow rates increase in the column, this in turns will increase the bubble coalescence producing a rise in the collection zone turbulences, consequently decreasing the collision possibility between the bubbles and the oily globules. Nevertheless, when the superficial liquid velocity is in a small value range (0.1 cm/s – 0.15 cm/s) the organics recovery has an increase with the increase in the liquid velocity, perhaps due to an increase of the retention of the air bubbles by the liquid flow in the collection zone. This effect can be noticed in fig. 11 where the organics recovery is plotted as a function of the superficial liquid velocity.

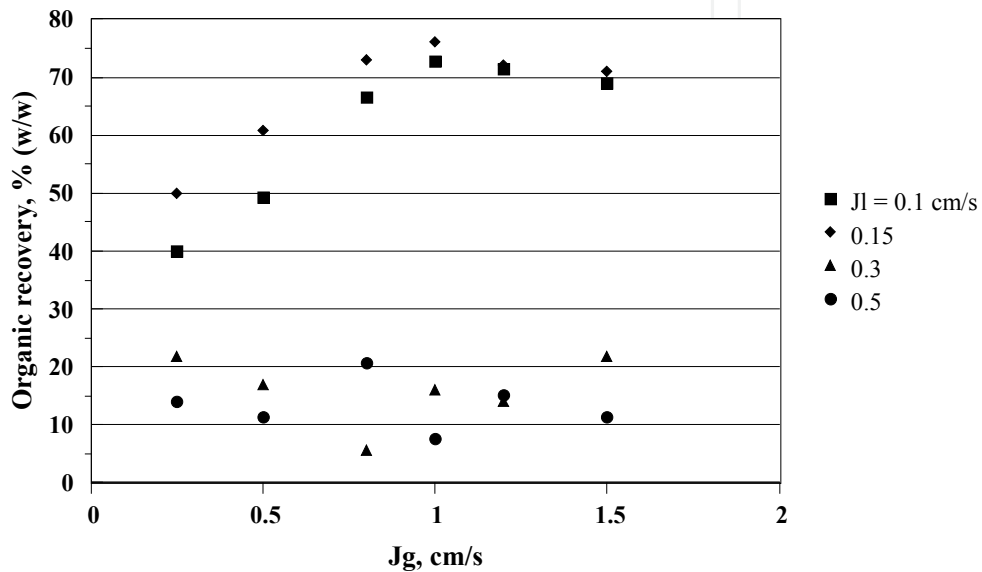


Figure 10. Organic recovery from water in the flotation column as the superficial gas velocity changes; the system is under different superficial liquid velocity.

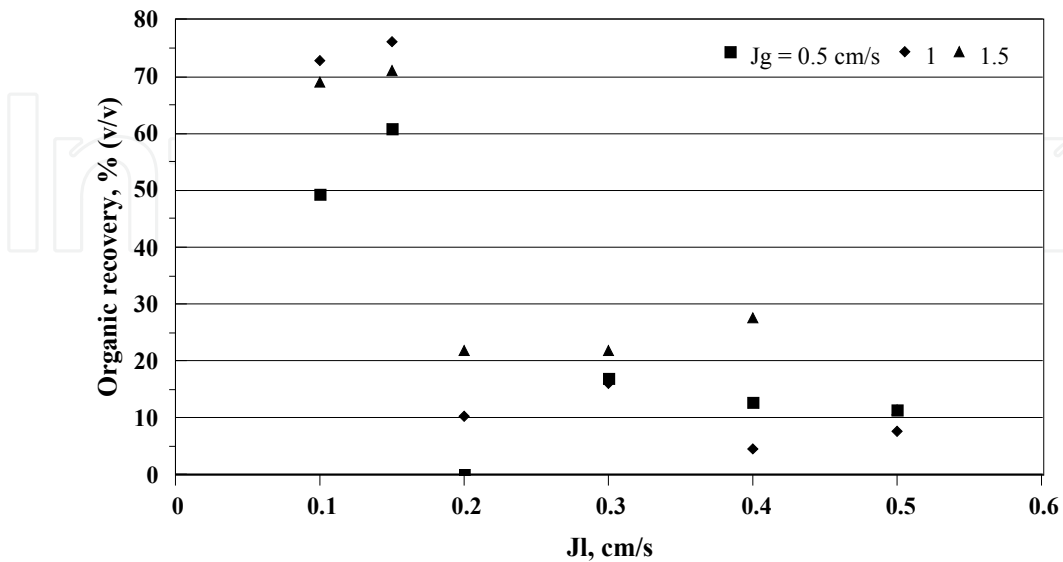


Figure 11. Organic recovery from water, reported in the flotation column concentrate, as a function of the superficial liquid velocity.

It can be observed that the de-oiling process efficiency is high when the superficial liquid velocity is kept below 0.2 cm/s, but above that value there is a drastic decline on the separation efficiency, this behaviour is observed in whole range of superficial gas velocities reported here. Also, it is thought that as the superficial liquid velocity increases in the collection zone of the flotation column, the possibility that small gas bubbles charged with hydrophobic organic materials are gone with the tailings flow out of the column, and for this reason, decreasing the organics recovery.

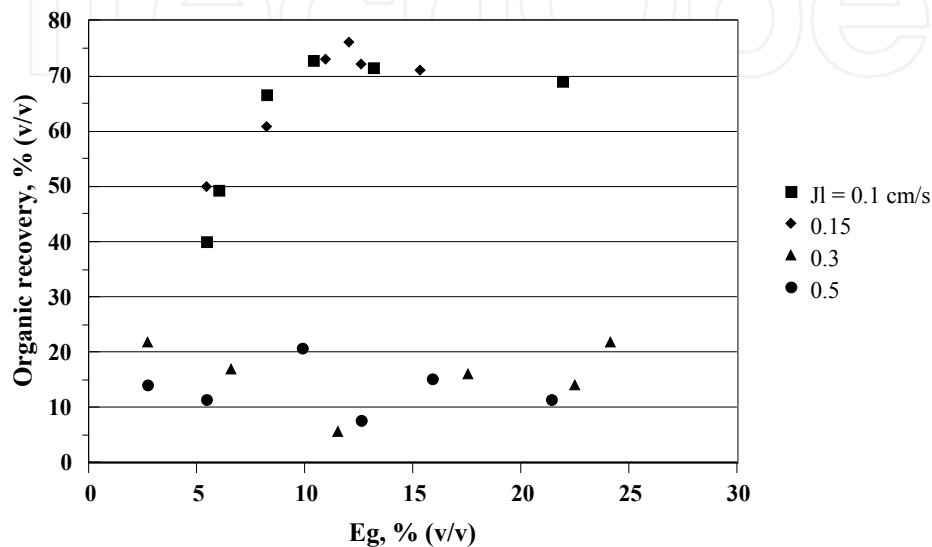


Figure 12. The effect of the superficial liquid velocity on the organic recovery/gas hold-up behaviour.

The experimental results plotted in fig. 12 suggest that large gas hold-up values are associated to small bubbles formation which will go down to the bottom of the flotation column because the effect of the downwards liquid stream; these experimental results support the impression that as the liquid flow rate increases the bubbles entrapment in the tailings stream also intensifies, producing low organic recoveries reported to the concentrate run. It can be noticed that under superficial liquid velocities above 0.15 cm/s the organic recovery in the concentrate ranges between 5% and 20%, which may be associated to large bubbles covered with the hydrophobic materials (which yields to such 5 to 20% organic recovery) and, therefore, most of the organic material collected by the gas bubbles is associated with the interactions with small bubble sizes. This idea is consistent with the hydrodynamic behaviour of gas bubbles moving in a liquid phase, since the oily globules present a lower density than the aqueous phase.

This explanation is supported by the gas bubble size estimates, from both image analysis and drift flux analysis, which are shown in Figure 13 in terms of the organic recovery in the concentrate.

The experimental bubble size estimates show the range of bubble dimensions is more constrained as the superficial liquid velocity is increased in the collection zone of the flotation column. This suggests that bubble-bubble coalescence is induced as the slip velocity among the phases (gas water counter-current flow) is increased.

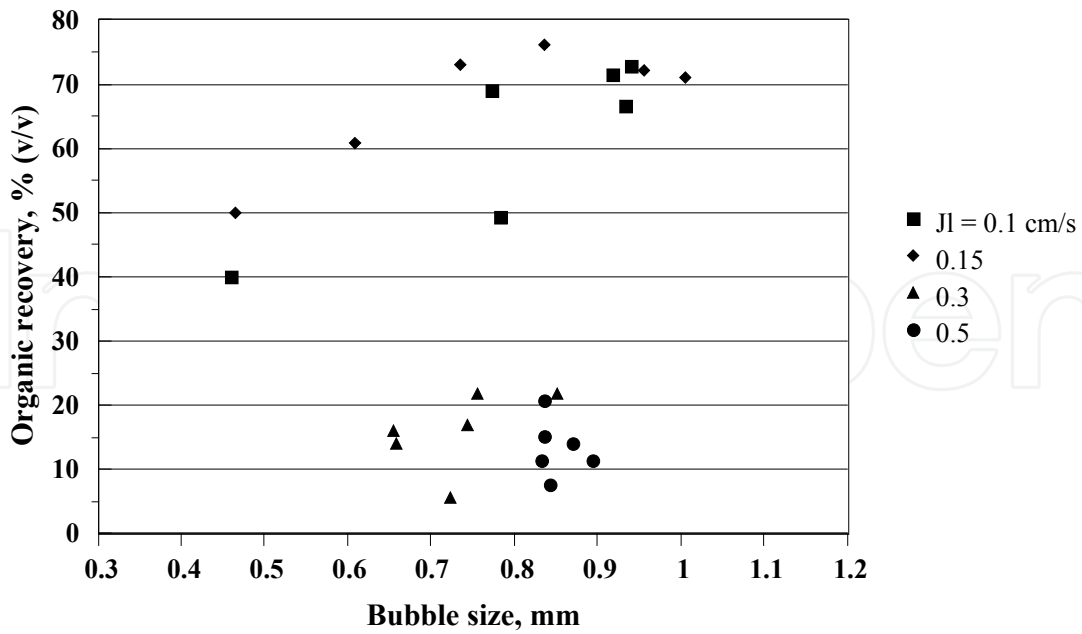


Figure 13. Effect of the bubble dimension on the recovery of organic floated.

Figure 14 presents the column flotation results on the water de-oiling process in terms of the organic recovery – superficial bubble surface flux behaviour. Under the lower values of the superficial liquid velocity in the collection zone of the column, it is very clear that the hydrophobic organic flotation increases when the gas surface area which flows in the flotation column increases.

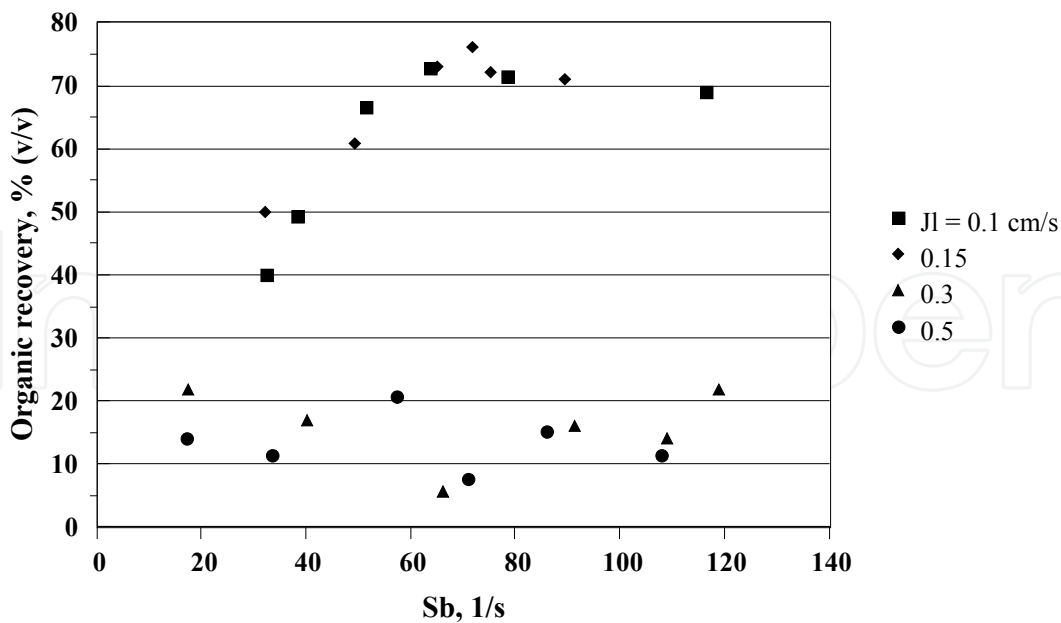


Figure 14. Behaviour of the organic recovery in concentrate with the change in the superficial bubble surface flux (Sb). The water de-oiling process in series stages of flotation columns. The water de-oiling process by column flotation was performed using a series of flotation stages. In this experience arrays of 2, 3 and 4 flotation column sequence were operated.

The experimental results and the estimates of the superficial bubble surface flux show that the hydrodynamic behaviour of the flotation column determines the separation efficiency and affects the relationship between the separation process and the available bubble surface area to perform the collection process. These experiences present that when the superficial liquid velocity is kept under the range between 0.1 and 0.15 cm/s, the change among the organic recovery and the superficial bubble surface flux follows a smooth pattern; however, when the superficial liquid velocity goes above 0.15 cm/s, the relationship between these process characteristics becomes erratic.

The experimental flotation columns array is schematically presented in fig. 15; this presentation shows that the residual water is fed into the first flotation column and the tailings from this column is used as the second column feed, and this arrangement is repeated up to four flotation columns.

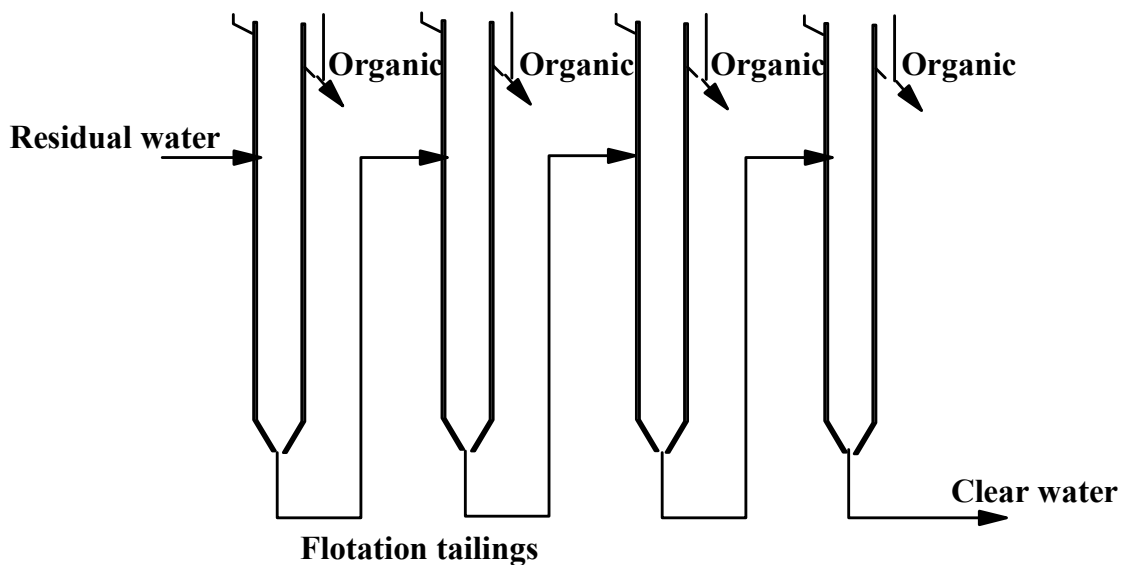


Figure 15. Experimental set up of flotation column series.

The experimental information shows that the de-oiling process can be performed effectively using a series of flotation columns. In this experience about 99% organic recovery is achieved using a series of four columns. The minimum residence time reported in order to achieve 99% organic recovery from the very stable water-oil (~40% oil) suspension is in the order of 100 minutes in a continuous four flotation columns operation [14].

2.3. Waste water treatment by crystallization – Cleaning of water contaminated with copper, lead, and nickel

It is well known the fact that although three quarters of this planet is occupied by water, not all is available for human consumption. 97% of this water is in oceans and seas whereas only 3% is called fresh water or sweet water. Of that 3%, the 77.6% is frozen polar ice, the 21.8% is groundwater, and only the 0.6% is available surface water for human consumption [15].

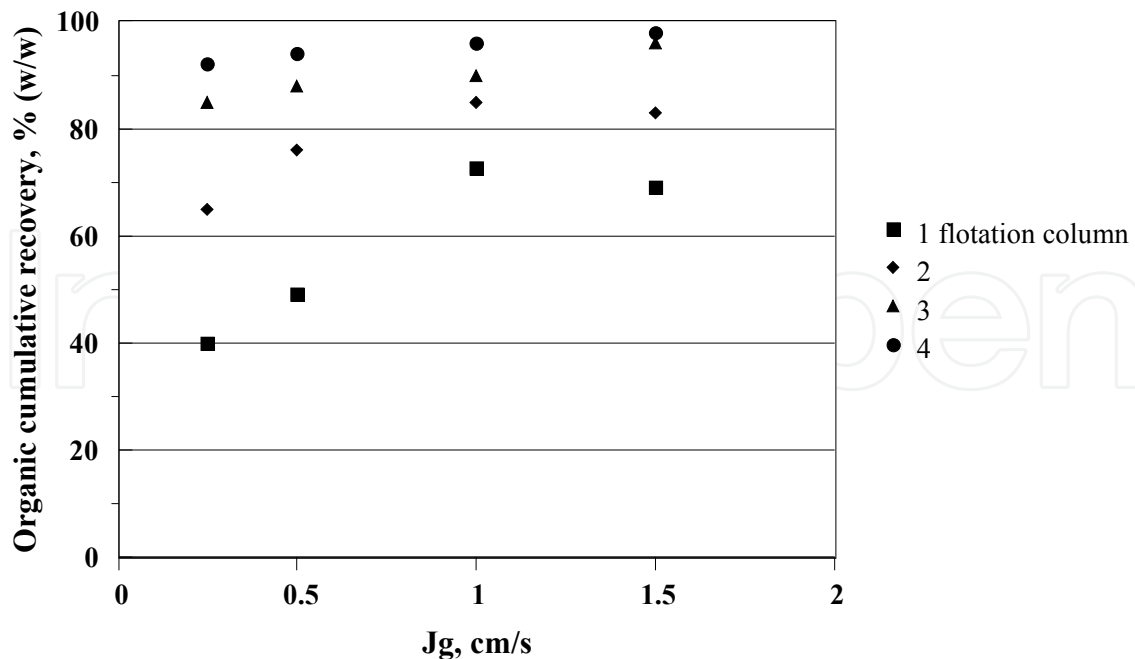


Figure 16. Experimental results of water de-oiling in one flotation column and a series of 2, 3 and 4 flotation columns.

According to the United Nations Industrial Development Organization (UNIDO), it is likely that in the year 2025 the industrial activity will consume twice as much water than at present; on the other hand, pollution may be multiplied by four due as well to this industrial activity [16]. Researchers at the Swiss Institute of Environmental Science and Technology recently reported that the rainwater that fall on the European Continent contains so many toxic pesticides dangerous for human consumption. In addition to acid rain, many other pollutants are deposited in water sources or streams, as in the third world, where 90% of the waste water is ending up in local rivers and streams [17]. The consumption of this contaminated water by the population leads to serious health problems such as gastrointestinal and cardiovascular disorders, malformations in newborns, among others. The World Health Organization (WHO) establishes the recommended levels of trace elements in drinking water (set for an average daily consumption), for both that help the body's metabolism as representing toxicity to humans. For instance, in the case of lead the recommended values are from 0.01 to 0.05 mg/l, whereas for copper is among 0.5 and 2.0 mg/l, depending of the government of each country [18, 19].

To solve the problem of contaminated effluents, are applied some processes in order to leave the water clear, colorless, odorless, and disinfected. The suspended solids, organic compounds, and pathogenic organisms, in most of the waste water treatment plants are removed; nevertheless, these processes do not eliminate the heavy metals dissolved in the effluent [20].

If the heavy metals are in solid state they may be extracted through a primary treatment (i.e., sedimentation or flotation) [21], or secondary (i.e., activated sludge) [22]. On the other hand, if heavy metals are in solution, the use of lagoons, hydroponic bed, activated zeolite

and membranes, phytoremediation, bird feathers, nanostructures, bioremediation, chemical crystallization, among others, have been proposed [23, 24, 25, 26, 27, 28].

Most of the processes mentioned above observe a certain limit as regards efficiency since the physicochemical aspects affecting such processes are not well understood, and the pollution problem is partially solved since the new "aggregate" with the removed contaminant remains as such.

This part of the chapter establishes from a thermodynamic point of view (pH, electrochemical potential, ionic strength, activity coefficient), the conditions to predict the formation of certain species (precipitated or dissolved) in distilled water contaminated with lead, copper, and nickel, and open to the atmosphere. The knowledge of the mechanisms of crystallization or chemical precipitation of the ionic species contribute to selectively agglomerate and separate the copper, nickel, and lead species in order to clean water contaminated with these heavy metals.

The role of heavy metals in reactions involving liquid-liquid and liquid-solid relationships is not enough studied yet. In the case of waste water treatment several research has been done although the mechanisms of precipitation of certain species and the selectivity of their capture is not clear [26, 27, 28]. For liquid-liquid, and solid-liquid systems, the interaction between species is ruled by the following expressions:

$$I = \frac{1}{2} \sum m_i z_i^2 \quad (1)$$

Where I is the ionic strength, which is a measure of the intensity of the electric field in the system [29, 30], m is the molality of i ; and z is the charge of the corresponding ion i (i represents every specie involved in a given reaction). In this work the involved species are the salts: $\text{Pb}(\text{NO}_3)_2$, CuSO_4 , and $\text{NiSO}_4 \cdot 6\text{H}_2\text{O}$, the water and the pH modifiers, H_2SO_4 , and KOH . The chemical activity is a corrected concentration [31], and physically is the actual amount of reagent that takes part during the reaction; in this case is the concentration of metallic ions in the media that affectively react. The average activity coefficient is calculated as follows:

$$\gamma_{\pm} = 10^{\left(A |z_+ z_-| \sqrt{I} \right)} \quad (2)$$

Being A the constant value from Debye-Hückel equation for liquid media and pressure of 1 atmosphere, $|z_+ z_-|$ is the absolute value of the sum of the electric charge of the dissolved ions. The activity a of given i species can be calculated according to:

$$a[i] = \gamma_i m_i \quad (3)$$

Where m is the molarity of the i species. In order to calculate the electrochemical potential, E_h , the equation proposed by Garrels [29] was applied:

$$E_h = E^\circ - \left(\frac{0.05916}{Z} \right) \log Q \quad (4)$$

Being E° the standard potential, Z the number of electrons participating during the reaction, and Q is the reaction quotient. E° can be calculated through the following expression:

$$E^\circ = \frac{-\Delta G^\circ}{ZF} \quad (5)$$

Where ΔG° is the Gibbs free energy of the corresponding reaction, and F is the Faraday constant ($96487 \text{ C/mol} = 23\,060.9 \text{ Cal/Vol}\cdot\text{mol}$). By applying the former equations there is possible to build $Eh - pH$ diagrams and to use them as tools to understand the conditions under which given ionic or precipitated species are chemically stable.

In this part of the chapter lead, nickel, and copper salts were dissolved in distilled water and physicochemical parameters such as ionic strength, activity coefficient, activity, and electrochemical potential were calculated, in a pH ranging from 3 to 13. Lead, nickel, and copper precipitates were identified and the corresponding formation reactions were established in order to build a Pourbaix diagram.

The obtained information makes possible at first to design a procedure to clean water contaminated with the heavy metals mentioned here through the route sedimentation-flotation or filtering-flotation. The experimental results also provide information regards deposited species on mineral surfaces during milling which affect the behavior of collectors during flotation decreasing its metallurgical performance.

2.3.1. Preparation of diluted solutions of Cu, Ni, and Pb in distilled water

Lead nitrate ($\text{Pb}(\text{NO}_3)_2$), copper sulphate (CuSO_4), and hexahydrated nickel ($\text{NiSO}_4 \cdot 6\text{H}_2\text{O}$) were dissolved separately and simultaneously in distilled water. The pH of the media was varied in 3,5,7,9,11, and 13. After 24 hours the precipitated solids were separated and analyzed through X-ray diffraction (XRD), and scanning electron microscopy (SEM) techniques. The remaining lead, copper, and nickel in every solution were quantified by atomic absorption spectroscopy (AAS) analysis. The pH was modified by adding sulfuric acid (H_2SO_4), and potassium hydroxide (KOH). The initial metal concentration in each solution was 40 ppm.

The chemical analysis of precipitates was carried out by X-ray diffraction (XRD), and scanning electron microscopy (SEM). On the other hand, the quantitative chemical analysis from liquids, were carried out by atomic absorption spectroscopy (AAS).

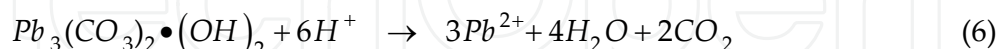
With the quantitative and qualitative chemical analysis data, the values of activity, activity coefficient, ionic strength, and electrochemical potential were calculated. The former information was used to calculate the corresponding transformation lines as function of the pH. The resulting equilibrium diagrams are shown below.

2.3.2. Precipitation of lead species

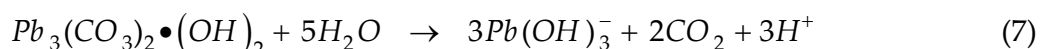
Visually the formation of lead precipitates starts at pH 3, although these solids are re-dissolved at pH 5. Lead crystals are formed again at pH 7, and finally the precipitates are

dissolved once more at pH 11. From XRD analysis at pH 3 the detected species are the lead sulfate ($PbSO_4$), and hydrated lead nitrite ($Pb(NO_2)_2 \cdot (H_2O)$), which indicates the decomposition and hydration of the salt originally dissolved. The precipitated solids at pH from 7 to 11 correspond to an hydroxycarbonate $Pb_3(CO_3)_2 \cdot (OH)_2$, also known as hydrocerusite.

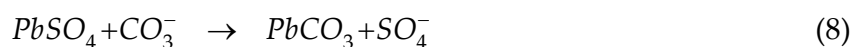
Taking into consideration that hydrocerusite forms under alkaline conditions, and in absence of ionic sulfate, the following reaction is suggested:



The re-dissolution of hydrocerusite is carried out according to the following reaction proposed by Pankow [31], and thermodynamically it occurs at pH 11.2:



On the other hand, the formation of carbonated species is explained by considering the replacement of sulfates or sulfites to carbonates in an open system to air, according the following reaction proposed by Azareño [32]:



In the case of the decomposition of lead sulfate:



From the above reactions it is possible to observe that the dissolution or precipitation of lead species just depends on pH. The Pourbaix diagram built according the calculated variables is shown in Figure 17. As known, in the following equilibrium diagrams the dashed lines represent the zone where aqueous species are stable; within these lines both the aqueous and precipitated species co-exist. For the copper case, the vertical lines correspond to the transformations shown in reactions (6), (7), and (9).

In light of the above, from pH up to 3.9, both ($PbSO_4$), and Pb^{2+} co-exist; whereas from pH 3.9 to 6 the all lead is dissolved. In the pH range from 6.0 to 11.2 the steady species are the Pb^{2+} and the $Pb_3(CO_3)_2 \cdot (OH)_2$. For pH larger than 11.2 the hydrocerusite is dissolved again and a lead hydroxide is formed.

According to the results from quantitative chemical analysis, the concentration of Pb^{2+} in the liquid media decreases because of the presence of lead precipitates at pH higher than 5, and the ionic lead increases again for pH higher than 11.

Table 1 shows the calculated values of activity for equations (6), and (9), as well as their Gibbs free energy, and the equilibrium pH. Thermodynamically the lead precipitation starts at pH 3.9 ($PbSO_4$), although visually it is noticed at pH 3. In the case of the $Pb_3(CO_3)_2 \cdot (OH)_2$, this visually starts at pH 7, whereas according to thermodynamics the precipitation

of such specie would initiate at pH 6. Differences between observations and calculations are due to human errors and it suggests the use of another technique (i.e., conductivity measurements) to detect accurately the moment at which the precipitation phenomena take place [33].

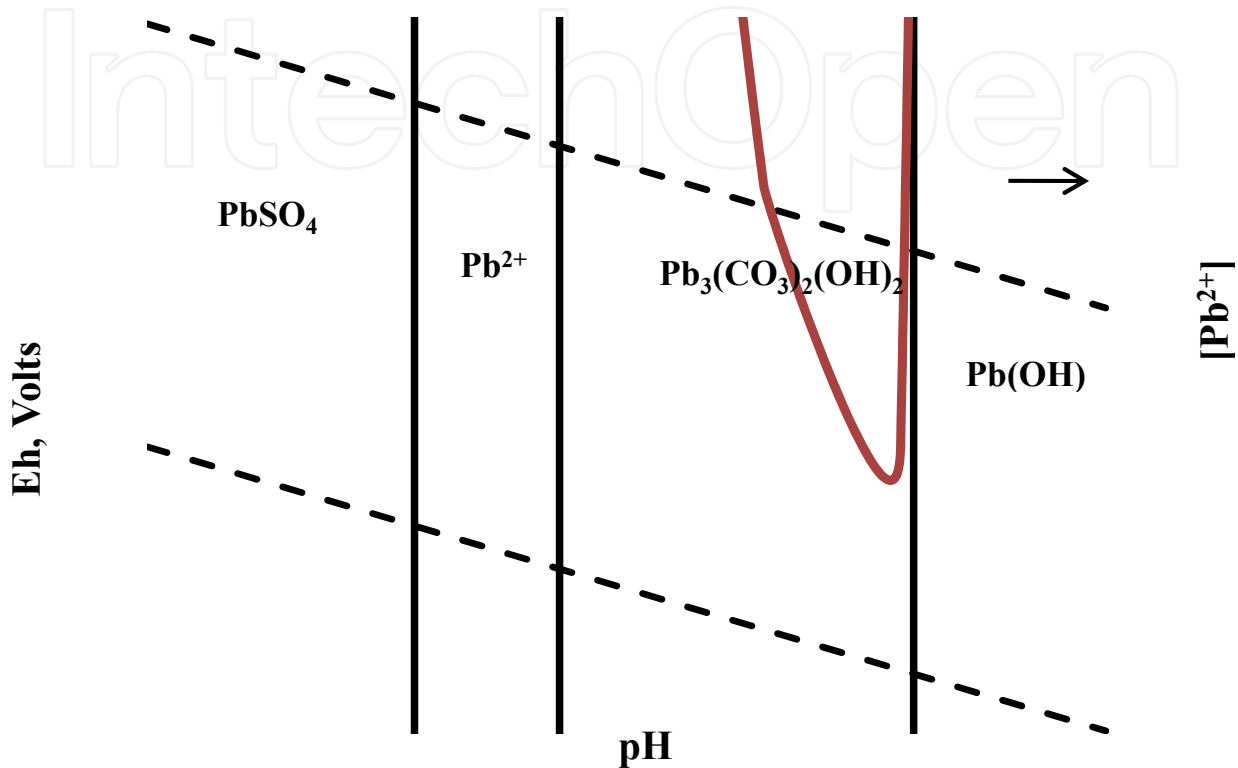


Figure 17. Transformation lines with changes on the metal concentration in the bulk solution. Pb – S – H₂O system.

Reaction	$a_{Pb^{2+}}$	ΔG° Reaction (Kcal/mol)	Equilibrium pH
$PbSO_4 + 2H^+ \rightarrow Pb^{2+} + H_2SO_4$	3.84E-04	-5975.14	3.9
$Pb_3(CO_3)_2(OH)_2 + 6H^+ \rightarrow 3Pb^{2+} + 4H_2O + 2CO_2$	2.14E-04	-24617.8	6.0

Table 1. Calculated values of activity of Pb^{2+} , Gibbs free energy, and the equilibrium pH for equations (6), and (9).

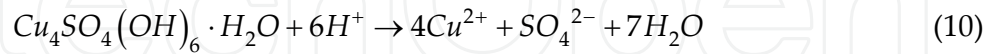
2.3.3. Precipitation of copper species

From qualitative DRX analysis the detected crystalline species are the hydrated copper hydroxisulphate ($Cu_4SO_4(OH)_6 \cdot H_2O$), cupric hydroxide ($Cu(OH)_2$), and cupric oxide (CuO). In the pH range from 3 to 5.5 there is not precipitation of any copper specie, whereas among pH 7.5 and 10.5 the three former species co-exist. From pH 5.5 to 7.5, and

10.5 to 13, the precipitated species are the hydrated copper hydroxysulphate, and the cupric oxide, respectively.

The solid, $\text{Cu}_4(\text{SO}_4)(\text{OH})_6 \cdot \text{H}_2\text{O}$, in a given pH transforms itself and co-exist with both the cupric hydroxide and the cupric oxide, and finally the cupric hydroxide transforms to cupric oxide at pH 10.5.

In the case of formation of the hexahydrated copper hydroxysulphate :



For the precipitation of the cupric hydroxide:



Being the formation of the cupric oxide defined by the following reaction:



The Pourvaix diagram for the Cu – S – H₂O system is shown in Figure 18, and Table 2: it shows the Gibbs free energy values for reactions (10), (11), and (12).

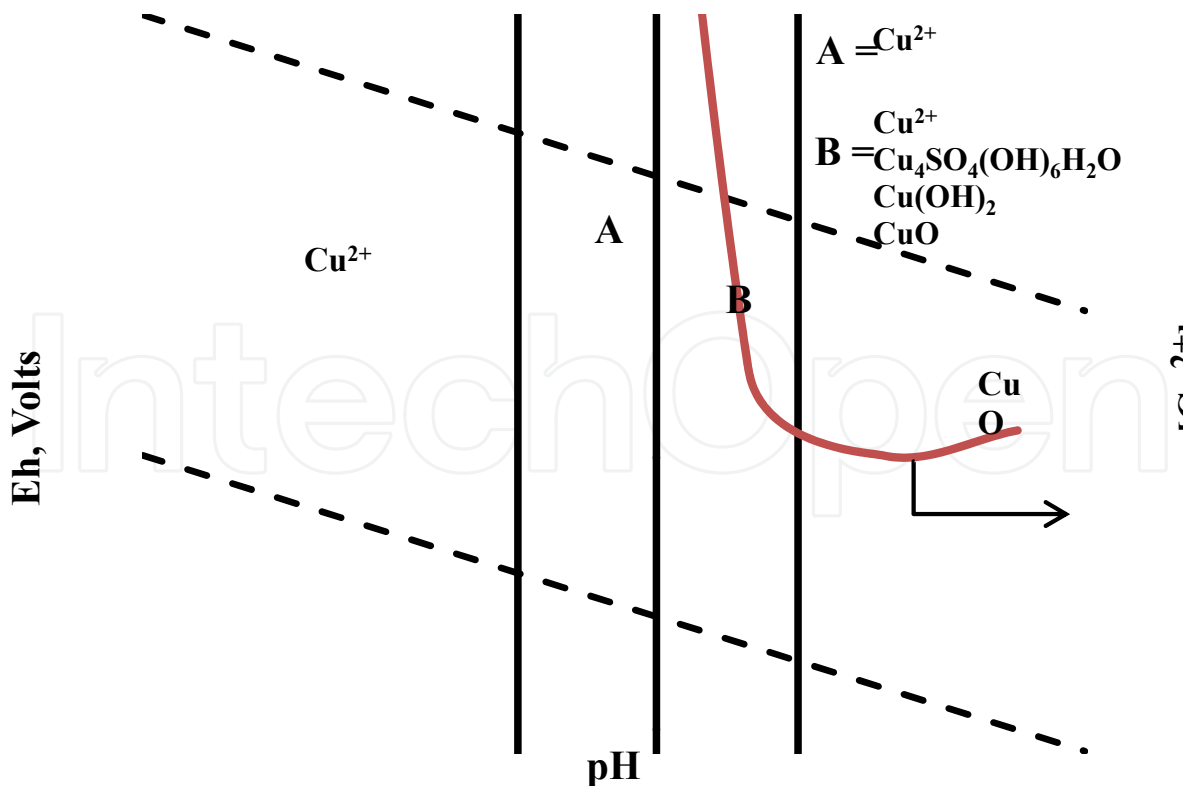


Figure 18. Pourvaix diagram for the Cu-SO₄-H₂O system. A and B means the liquid and solid species that co-exist in a respective region.

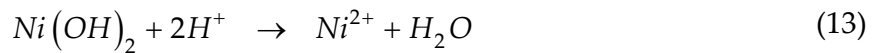
Reaction	$a_{Cu^{2+}}$	ΔG° Reaction (Kcal/mol)	Equilibrium pH
$Cu_4SO_4(OH)_6 \cdot H_2O + 6H^+ \rightarrow 4Cu^{2+} + SO_4^{2-} + 7H_2O$	8.00E-04	193.6	5.6
$4Cu(OH)_2 + 2H^+ + CuSO_4 \rightarrow CuSO_4(OH)_6 \cdot H_2O + Cu^{2+} + H_2O$	4.08E-05	176.37	7.6
$4CuO + CuSO_4 + 3H_2O + 2H^+ \rightarrow Cu_4SO_4(OH)_6 \cdot H_2O + Cu^{2+}$	4.08E-05	143.4	9.7

Table 2. Activity, Gibbs free energy, and equilibrium pH values for reactions (10), (11), and (12).

2.3.4. Precipitation of nickel species

In this case and according to the DRX analysis the only detected species was the nickel hydroxide ($Ni(OH)_2$). Visually the precipitation of such species is detected at pH 9; although, thermodynamically the nickel hydroxide starts forming at pH 7.6. Figure 19 shows the Eh-pH diagram for the Ni-SO₄-H₂O system.

From the above information the proposed reaction is as follows:



The corresponding thermodynamic values are shown in Table 3. Sean et al., [20], Chanturiya et al., [21], Liu [22], Shigehito et al., [23], and Guo-riu Fu [24], reported the precipitation of two nickel phases named α – nickel hydroxide, and β – nickel hydroxide, within the pH range established in this work. These species were detected by using both: XRD and IR analysis techniques.

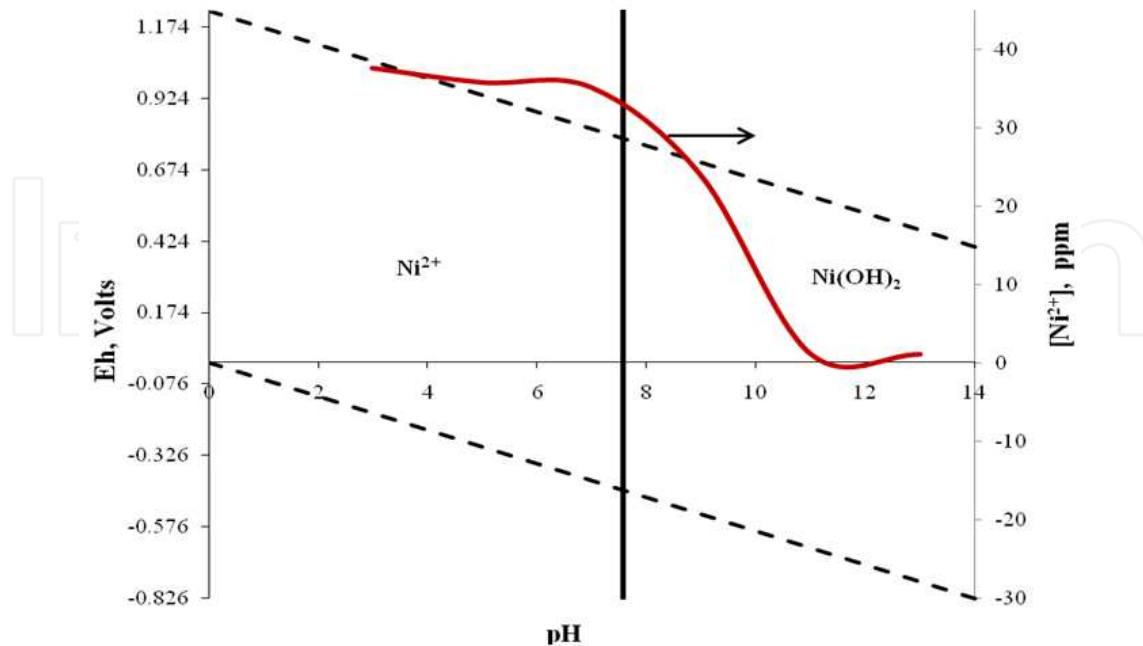


Figure 19. Pourbaix diagram for the Ni – SO₄ – H₂O system. Changes on concentration of the ionic nickel are included.

Reaction	$a_{\text{Cu}^{2+}}$	ΔG° Reaction (Kcal/mol)	Equilibrium pH
$\text{Ni}(\text{OH})_2 + 2\text{H}^+ \rightarrow \text{Ni}^{2+} + \text{H}_2\text{O}$	4.47E-03	-17447.1	7.57

Table 3. Activity coefficient, Gibbs free energy, and equilibrium pH for reaction (13).

2.4. Selective precipitation of copper, nickel, and lead

With all the above information it is possible to design a cleaning route for water contaminated with lead, copper and nickel. By adjusting the pH of the media selectively any of the metals can be precipitated and then separated by filtration or sedimentation.

Lead, copper, and nickel salts were simultaneously dissolved in distilled water. The amount of every salt was adjusted to fix the initial concentration of every metal at 160 g/l.

According to the experimental data and the thermodynamic calculations, each metal can be selectively precipitated and removed from the contaminated effluent. After each pH adjustment of the liquid, the solids were separated by centrifugation. The proposed procedure is as follows:

- At pH values up to 4 the only precipitated specie is the lead sulfate (PbSO_4), remaining in the liquid media both the nickel and the copper. Figure 20 shows the XRD analysis of the solids crystallized under pH 3.

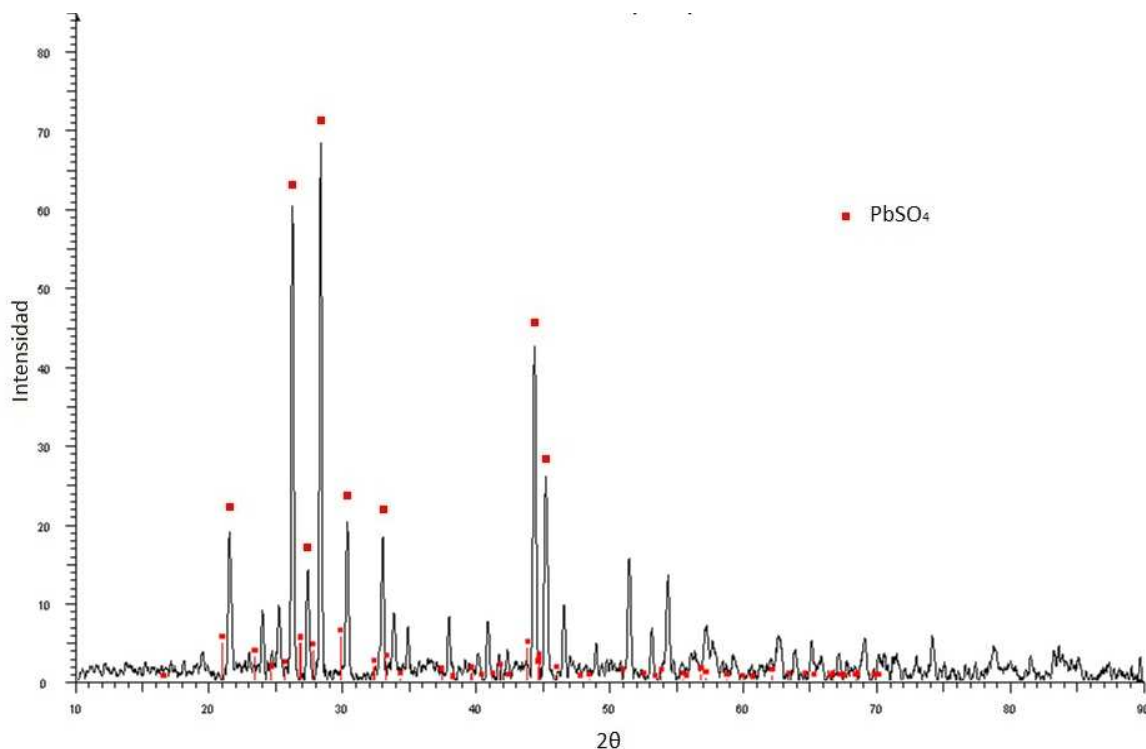


Figure 20. XRD analysis for solids precipitated at pH 3. Experimental results for the case of lead, copper, and nickel salts simultaneously dissolved in distilled water.

- b. By keeping the pH at 7.5, the copper species will precipitate as hydroxysulphate, and only the nickel is expected to remain in solution. Figure 21 shows the XRD analysis of the solids precipitated at this stage. Considering that the pH of equilibrium for the Ni-H₂O system is 7.6, it seems normal to observe the onset of precipitation of some nickel species.

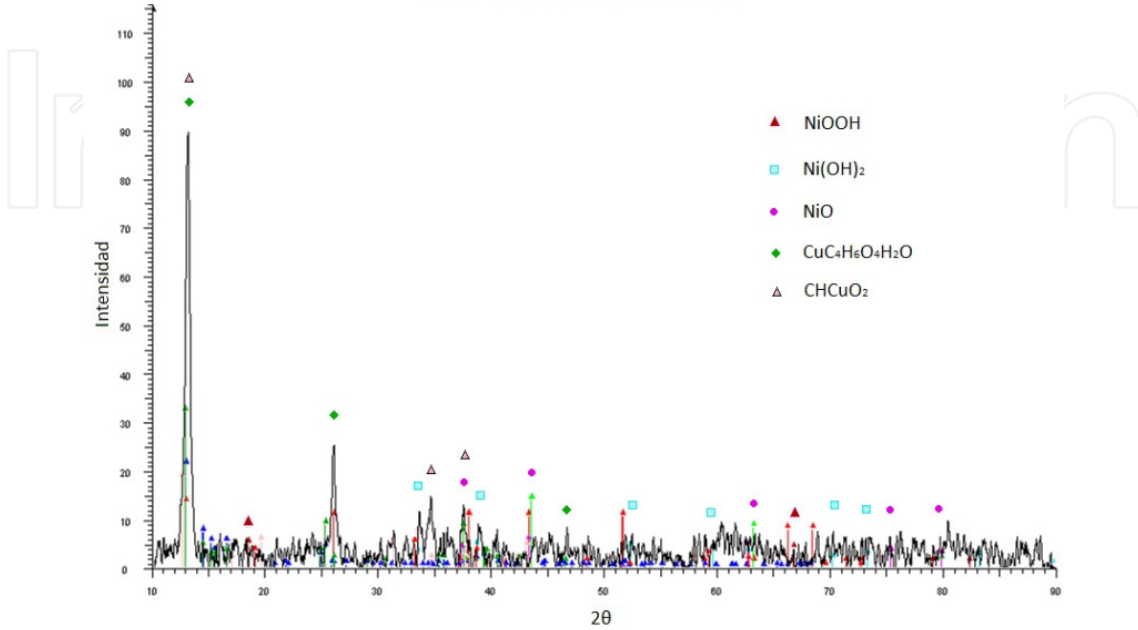


Figure 21. XRD analysis for solids precipitated at pH 7.5. Experimental results for the case of lead, copper, and nickel salts simultaneously dissolved in distilled water.

- c. Finally, if the pH of the liquid is fixed at values larger than 10, the nickel will precipitate as hydroxide. Figure 22 shows the XRD result after fixing the pH at 11.

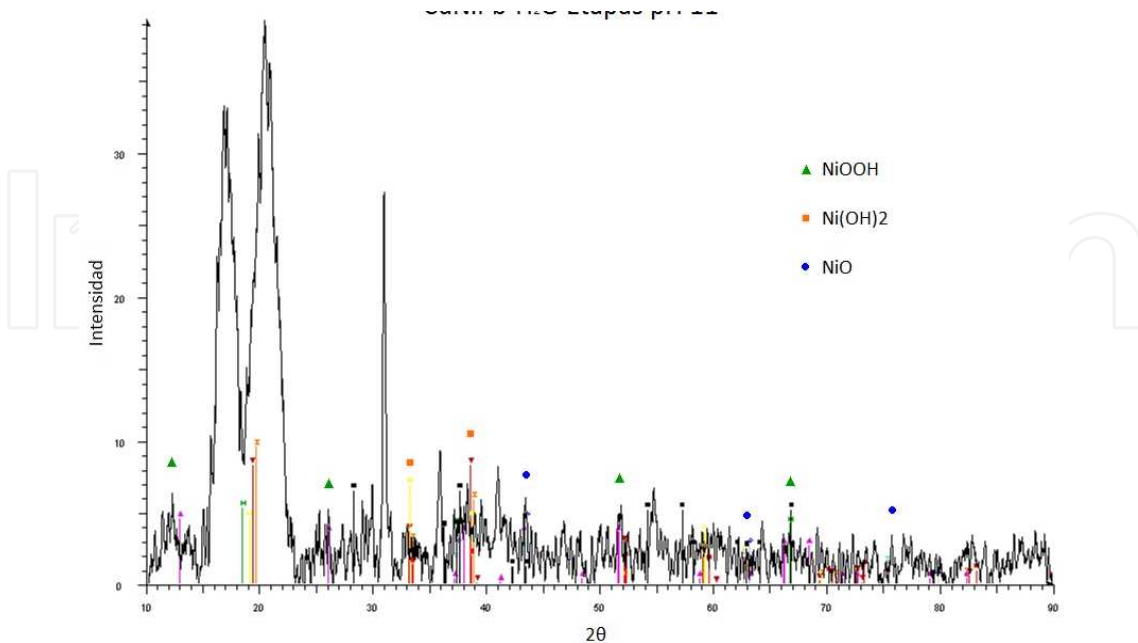


Figure 22. XRD analysis for solids precipitated at pH 11. Experimental results for the case of lead, copper, and nickel salts simultaneously dissolved in distilled water.

2.5. Waste water treatment de-oiling by using microorganisms

The biological treatments are procedures for cleaning waste water effluents; they have in common the use of microorganisms (i.e., bacteria), to carry out the removal of undesirable components of the water, using the metabolic activity of such microorganisms. The traditional application is the removal of biodegradable organic matter, either soluble or colloidal, and the elimination of compounds containing nutrients (nitrogen and phosphorous). The following describes an experimental procedure, carried out at laboratory level, to eliminate vegetable oils, first from a synthetic emulsion and then, from an industrial effluent. The microorganisms tested here, are both aerobic and nonpathogenic. The bioreactor used was a flotation cell made of transparent acrylic material.

2.5.1. Determining the lipolytic capacity of microorganisms

With the appropriate conditions for the growth of the bacteria colony (pH, temperature, dissolved oxygen, surface tension, and nutrients), it was possible to quantify the lipolytic capacity of the microorganisms: *Candida Kefir*, *Candida Parapsilosis*, *Pseudomonas Fluorescens*, *Bacillus Cereus*, and *Bacillus Coagulans*, individually and in bulk. Since the purpose of this stage of the work was to establish the lipolytic character of the above mentioned microorganisms, the measurements of residual oil in water were carried out at the beginning and at the end of the experimental digestion. The experimental results are shown in Table 4.

SAMPLES	RESIDUAL OIL (g/l)	RESIDUAL OIL (%)
Undigested sample	0.241	100
<i>Candida Kefir</i>	0.233	96.5
<i>Candida parapsilosis</i>	0.023	9.78
<i>Bacillus cereus</i>	0.059	24.5
<i>Pseudomonas fluorescens</i>	0.005	2.3
<i>Bacillus coagulans</i>	0.019	7.9
Bulk	0.023	94.7

Table 4. Residual oil in the synthetic emulsion after microbial action.

From table 1 the microorganism with higher lipolytic capacity is the *Pseudomonas fluorescence*, leaving only 2.3 % of residual oil in the emulsion. The same experimental results expressed in terms of the biomass developed (growth of colony) is shown in Table 5. As can be observed, the amount of biomass increases with the oil removed from the emulsion, due to the amount of nutrients (lipids) ingested by the microorganisms.

The microorganism with more biomass developed during the ingestion of lipids was the *Pseudomonas fluorescens* (253.5%), followed by the *Bacillus coagulans* (197.9%), and at the end appears the *Candida parapsilosis* (178%). Table 6 shows the variations in pH, temperature, and dissolved oxygen, monitored during this first stage of experimentation and corresponding to the particular case of the *Pseudomonas fluorescens*. The entire experiment finished after 132 hours.

SAMPLES	BIOMASS (g/l)	BIOMASS (%)
Undigested sample	0.247	100
<i>Candida Kefir</i>	0.328	132.7
<i>Candida parapsilosis</i>	0.344	139.2
<i>Bacillus cereus</i>	0.440	178.0
<i>Pseudomonas fluorescens</i>	0.626	253.5
<i>Bacillus coagulans</i>	0.489	197.9
Bulk	0.329	158.5

Table 5. Development of biomass in the degradation of a synthetic emulsion.

Sampling (hrs)	pH	Temperature (°C)	Surface Tension (dyn/cm)	Dissolved Oxygen (mg/l)	Residual Oil (%)	Biomass (%)
0	5.9	17	36.8	6.4	100	100
12	5.7	21	38.1	6.6	95	104
24	5.1	18	36.6	7	87	100
36	4.7	20	36.5	6.8	81	102
48	4.6	18	36.6	7	71	105
60	4.4	20	36.9	6	67	108
72	4.3	17	38.9	6.5	58	101
84	4.3	19	36.9	6.1	55	111
96	4.1	17	41.3	5.9	47	112
108	4.1	20	41.2	6	41	116
120	4.1	18	41.5	6	33	127
132	4.1	21	42.1	6	23	146

Table 6. Experimental results after digestion of the synthetic emulsion by the microorganism *Pseudomonas fluorescens*.

From table 6 the pH of the system decreased during the first 100 hours of the experiment. After this time, the pH of the emulsion remained constant at pH 4.1. This acidification is caused by the rupture of triglycerides, releasing fatty acids and glycerol, together with the carbonic acid formed when water combines with the carbon dioxide from the bacterial metabolism. Regarding the surface tension of the emulsion, this increases with the amount of lipids ingested by the microorganisms, because of the ionic species eliminated from the emulsion, increasing the cohesive forces of the fluid [39]. This increase in the surface tension value is more evident after 96 hours of starting the cleaning process of the synthetic emulsion.

The increase in the surface tension coincides with the increase in the biomass after the 96 hours above referred. As shown in table 6, inoculation lasted approximately 80 hours, and the bacterial colony growth remained. Then after 52 hours, the exponential growth phase of the colony is observed, increasing 45% compared with the initial biomass. It is not observed a decrease in the biomass because there are still nutrients (oil) to degrade by the microorganisms.

The behavior of the dissolved oxygen (DO) in the emulsion also has a direct relationship with the colony growth; during the inoculation phase, the DO practically remains constant (~ 6.6 mg/l), then there is a decrease in the amount of dissolved oxygen by the growth of the colony of microorganisms.

2.5.2. De-oiling of an industrial effluent

A sample of the effluent from an edible vegetable oils factory was collected. The amount of oil, quantified according the Soxhlet technique [40], was of 41.45 mg/l, which is above the maximum permissible value for the environmental standards. The initial pH of the sample was 5.6 and this value does not affect the growth of the *Pseudomonas fluorescens* bacteria, since this microorganism is naturally acidophilus. Table 7 shows the measured variables to the original sample.

Characteristic	Result
pH	5.8
Surface Tension (dyn/cm)	37.9
Dissolved Oxygen (mg/l)	0.35
Oil content (mg/l)	41.5

Table 7. Characteristics of an effluent from an edible vegetable oils factory.

A set of experiments were run by using a transparent acrylic plexiglass cell as biological reactor (30 cm by side and 40 cm in height), with 4 taps properly located to adjust 4 sensors for measuring continuously: pH, temperature, dissolved oxygen, and surface tension of the system. A bubble generator (made of filter cloth) was installed at the bottom of the reactor. The air feed to the cell was measured and controlled through a mass flow controller. The system was operated under stationary regimen, and open to the atmosphere. Table 4.5 shows the experimental variables applied in this particular research.

Variable	Value
Volume of emulsion fed to the cell	7.0 liters
pH	5.6
Air fed to the cell	25 l/min
Microorganism	<i>Pseudomonas fluorescens</i>
Sampling time	Every 48 hours
Volume of each sample	20 ml
Test duration	8 days

Table 8. Experimental conditions for de-oiling of an industrial effluent using a laboratory biological reactor.

Figure 23 shows changes in pH during the bio-treatment of the industrial sample. As can be observed the pH of the liquid media increases with the time (from 5.6 to 8.5). This is associated with the stressful conditions in the system: the special nutrients are depleted,

waste products accumulate, bacterial overpopulation occurs (causing high demand of oxygen for aerobic metabolism), conditions that limit the growth colony and cause cell death.

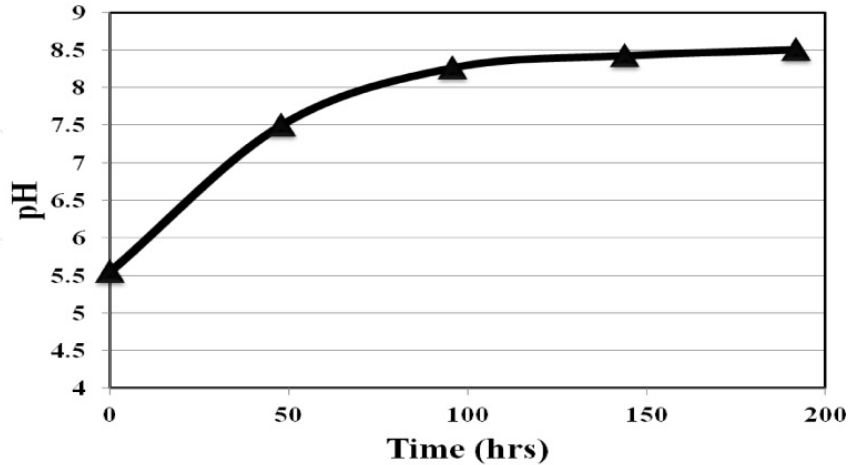


Figure 23. Changes in pH during the bio-treatment of the industrial effluent. *Pseudomonas fluorescens* bacteria were used to degrade oil.

Even the pH of the media begins to be unsuitable for cell growth. At this time there are more dead than alive bacteria, then the scarcity of nutrient sources (sugars and lipids), the protein degradation process of the bacteria begins, and generates ammonia as degradation product. This process provides organic nitrogen sources as nutrient which transforms the system into alkaline, increasing the pH value [41].

On the other hand, as in the case of the synthetic emulsion, the surface tension of the effluent increases with the time, because of the amount of lipids ingested by the microorganisms. As mentioned above, the cohesive forces of the fluid increase because of the ionic species eliminated from the emulsion (see Figure 24).

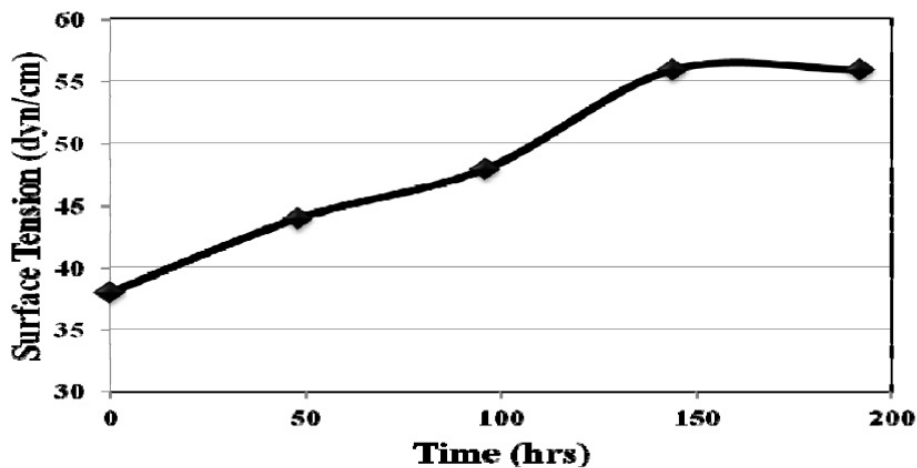


Figure 24. Changes in the surface tension of the effluent with the time, due to the increment in the amount of lipids digested by the microorganisms.

The lipolytic activity of the microorganisms is presented in Figure 25. The initial concentration of fat in the effluent was equal to 41.5 mg/l (taken as 100%); at 48 hours after initiation of the experiment the oil content in the emulsion decreased to 34.2 mg/l (82.4%); at 96 hours of incubation, was reached a concentration below 10 mg/l (24%), and finally, after 144 hours of the vegetable oil content in the effluent was 4.6 mg/l (11%) and remained constant from this point.

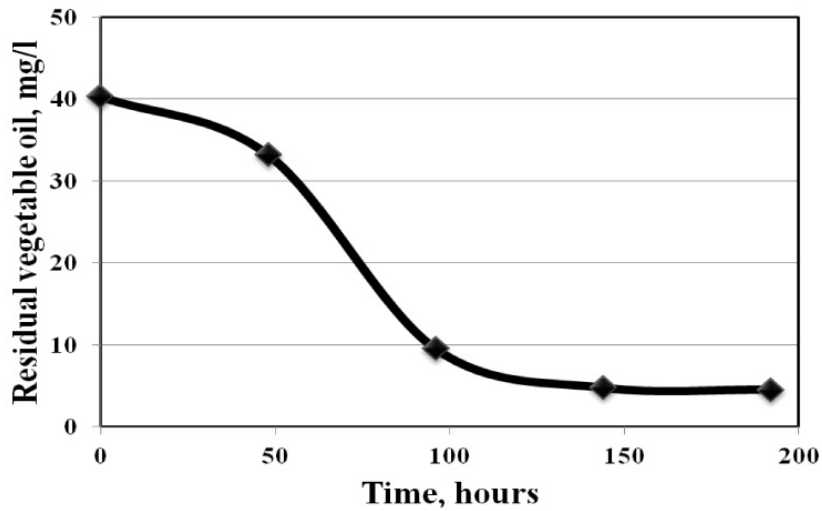


Figure 25. Variations of the vegetable oil content in the industrial effluent treated by the microorganism *Pseudomonas fluorescens*.

The constant trend in the last two experimental points, shown in figure 3, coincides with the trends of both: pH and surface tension, shown in figures 1 and 2, respectively, which also agrees with the behavior of the biomass in the last two points of sampling, as can be seen in Figure 26.

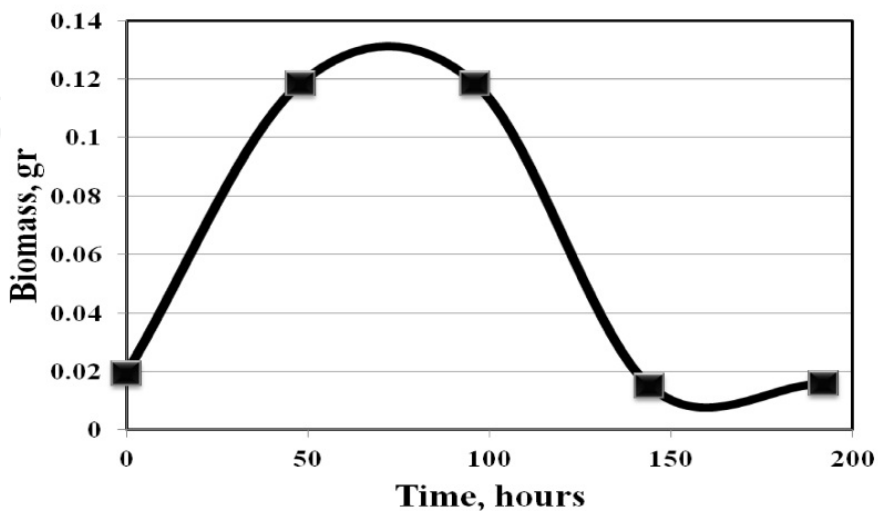


Figure 26. Biomass development (*Pseudomonas fluorescens*) during the degradation of an industrial effluent.

Is observed in figure 26 that biomass increased five times their initial concentration in a period of 48 hours of incubation, this development continued until approximately 100 hours of testing; this period matches with the maximum lipolytic degradation in the effluent. At this time the fat concentration of the effluent reached the lowest value (4.6 mg/l); the bacterial growth was limited to the shortage of nutrients and metabolic waste buildup in the effluent.

2.6. Conclusions

The information derived from the set of experiments conducted to establish the feasibility of using flotation devices in non-mineral systems, such as waste water treatment, can be used to set the following conclusions:

The experimental information shows that the de-oiling process can be performed effectively using a series of flotation columns. In this experience about 99% organic recovery is achieved using a series of four columns. The minimum residence time reported in order to achieve 99% organic recovery from the very stable water-oil (~40% oil) suspension is in the order of 100 minutes in a continuous four flotation columns operation.

Aerated flotation cells can be used as oxygen suppliers to aerobic nonpathogenic microorganisms (i.e., *pseudomonas fluorescens* bacteria), used during the biological treatments for cleaning waste water effluents; these microorganisms degrade the fat components of the water (either ionic or colloidal), using their metabolic activity. The experimental results shows that through these bacteria, around the 90% of the vegetable oil content in the effluent can be removed.

On the other hand, by precipitating heavy metal ions, it is possible to design a process for cleaning waste water contaminated with heavy metals (i.e., lead, copper, and nickel), through a sedimentation-flotation route.

The thermodynamic al analysis of the metal-water systems (activity, activity coefficient, ionic strength, electrochemical potential), allows accurately predict the crystallization of the ionic species under controlled conditions of temperature and pH.

The experimental results shows that these data converge well enough with the thermodynamic calculations for dissolved or precipitated lead species, being possible the selective precipitation of the three metals tested here, and leaving the water without any kind of metal, ionic or solid.

Author details

Ramiro Escudero*, Francisco J. Tavera and Eunice Espinoza
*Instituto de Investigaciones Metalúrgicas, Universidad Michoacana de San Nicolás de Hidalgo,
 Morelia, Michoacán, México*

* Corresponding Author

Acknowledgement

The authors deeply appreciate the support given to this investigation to the Universidad Michoacana de San Nicolas de Hidalgo, and the Mexican Government through the National Council for Science and Technology.

3. References

- [1] Sebba, F. 1962. Ion Flotation. Elsevier Publishing Co., New York.
- [2] Doyle, F. M. 2003. Ion flotation – its potential for hydrometallurgical operations. *Int. J. Miner. Process.*, 72, pp. 387 – 399.
- [3] Finch, J. A., Dobby, G. S. 1990. Column Flotation. Pergamon Press, Oxford.
- [4] Lara, R. H. C., Cruz, R. G., Monroy, M. G. F. 2005. Mecanismos de la alteración de la galena asociados al efecto ambiental en medios calcáreos. Artículo presentado en el XL Congreso Mexicano de Química, Sociedad Química de México, 25 – 29 de Septiembre, Morelia, México.
- [5] Tavera, F. J., Reyes, M., Escudero, R., Patiño, F. 2010. On the treating of lead polluted water: flotation of lead colloidal carbonate. *J. Mex. Chem. Soc.*, vol. 54 (4), pp. 204 – 208.
- [6] Tavera, F. J., Escudero, R., Uribe, A., Finch, J. A. 2000. Ni – DETA flotation in aqueous media: application of flotation columns. *AFINIDAD*, LVII (190), pp. 415 – 423.
- [7] Tavera, F. J., Gomez, C. O., Finch, J. A. 1996. A novel gas hold-up probe and application in flotation columns. *Trans. Instn. Min. Met.*, 105 (C), pp. 99 – 104.
- [8] Maxwell, J. C. 1892. A Treatise of Electricity and Magnetism. 3rd Edition, 1 (II), Chapter IX, Oxford University Press, London, pp. 435 – 449.
- [9] Tavera, F. J., Gomez, C. O., Finch, J. A. 1998. Conductivity flow cells for measurements on dispersions. *Can. Met. Quart.*, 37 (1), pp. 19 – 25.
- [10] Escudero, R. 2000. Characterisation of rigid porous spargers by permeability and its relevance to scaling-up. Ph. D. thesis, McGill University, Montreal, Canada.
- [11] Tavera, F. J., Escudero, R., Finch, J. A. 2001. Gas hold-up in a flotation column: laboratory measurements. *Int. J. Miner. Process.*, 61, pp. 23 – 40.
- [12] Gorain, B. K. 1997. The effect of bubble surface area flux on the kinetics of flotation and its relevance to scale – up. Ph. D. thesis, University of Queensland, Australia.
- [13] Levenspiel, O. 1972. Chemical reaction engineering. 2nd ed., McGraw Hill, Inc., New York.
- [14] Tavera, F. J., Escudero, R., Sánchez, A. 2004. Treating of water polluted with organics in flotation columns. Proceedings of the International Symposium on Environment; ISBN 970-703-293-6, Morelia, Mexico, pp. 95 – 105
- [15] Grover V. I. (2006). *Water: global common and global problems*. Science Publishers.
- [16] [www.unido.org]
- [17] Barlow M., & Clarke, T. (2004). *Oro azul: las multinacionales y el robo organizado de agua en el mundo*. Ed. Paidós.
- [18] Alvez, Z. C. (1995). Qualidade da água. Meio Ambiente por inteiro. *Jornal da Secretaria Municipal do Meio Ambiente* (1), 7.

- [19] www.who.int/
- [20] Crites, R., and Tchbanoglous, G. (2004). *Tratamiento de Aguas Residuales en Pequeñas Poblaciones*. (M. Camargo, L. P. Pardo, & G. Mejía, Trans.) Mc Graw Hill.
- [21] Metcalf, and Eddy, INC. (1994). *Ingeniería Sanitaria, tratamiento, evacuación y reutilización de aguas residuales* (Tercera Edición ed.). (J. d. Montsoriu, Trad.) Ed. Labor.
- [22] Celis Hidalgo, J., Junod Montano, J., and Sandoval Estrada, M. (2005). *Recientes Aplicaciones de Depuración de Aguas Residuales con Plantas Acuáticas, Teoría* (Vol. 14).
- [23] Alba Elias, F., Vergara Gonzalez, E. P., Ordieres, J. B., Martinez de Piston, F., González Marcos, A., and Ortiz Marcos, I. (s.f.). Tratamiento de aguas contaminadas con metales pesados empleando compost usado de champiñon como agente bioregenerador. 16.
- [24] López Martínez, A., Cuapio Ortiz, L., Cárdenas Puebla, S., Balcazar, M., Jauregui, V., and Bonilla Petriciolet, A. (2007). Determinación de Concentración de Cr y Cd Adsorbido por Plumitas de Pollo. *Tesis de Maestría*. (I. T. Aguascalientes, Ed.)
- [25] Soto, E., Miranda, R. D., Sosa, C. A., and Loredó, J. A. (2006). Optimización del Proceso de Remoción de Metales Pesados de Agua Residual de la Industria Galvánica por Precipitación Química. *Información Tecnológica*, 17 (2), 33-42.
- [26] Aksu S. and Doyle F. M., Potential-pH Diagrams for Copper in Aqueous solutions of various organic complexing agents, *Electrochemical Society Proceedings* Vol. 2000(14), 258-269 (2000).
- [27] Reyes Pérez M. 2005, Tratamiento continuo, de aguas contaminadas con Cu y Pb, por flotación iónica en celdas con dispersores porosos; efecto de las propiedades de la dispersión aire-líquido en la separación, Tesis de maestría, IIM, UMSNH, (2005).
- [28] Barakat M. A., Removal of Cu (II), Ni (III) and Cr(III) Ions from Wastewater Using Complexation - Ultrafiltration Technique, *Journal of Environmental Science and Technology*, Vol. 1 (3): 151-156, (2008).
- [29] Garrels, R. M. and Christ, C. L., *Minerals, Solutions, and Equilibria*, Harper & Rowe, N. Y. 450pp, (1965).
- [30] Cisternas L. A., *Diagramas de fases y su aplicación*, Reverte, (2009).
- [31] Pankow J. F., *Aquatic chemistry concepts*, CRC Press, (1991).
- [32] Azareño O.A., Núñez J. P., Figueroa L. A., León D. E., Fernández S. S., Orihuela S. R., Caballero R. M., Bazán R. R., and Yi Choy A. S. Flotación de Minerales Oxidados de Plomo. *Revista del Instituto de Investigación de la Facultad de Ingeniería Geológica, Minera, Metalúrgica y Geográfica*. Vol. 5 (10), 34-43, (2002).
- [33] Tavera F. J., Colwell D., Escudero R., and Finch J., (2000). Estimation of Gas Holdup in Froths by Electrical Conductivity: Application of the Standard Addition Method. *Revista de Química Teórica y Aplicada AFINIDAD*, Barcelona Vol. 57(486), 139-142, España, Abril.
- [34] Sean R. S., and Thomas S.D. (2002). Raman Spectroscopy of $\text{Co}(\text{OH})_2$ at High Pressures: Implications for Amorphization and Hydrogen Repulsion. *Physical Review*. Vol. 66 B, pp 134301-1 – 134301-8.
- [35] Chanturiya, V.A., Matveeva T.N., and Lantsoba L.B. (2003). Investigation into Products of Dimethyl Dithiocarbamate and Xantate Sorption of Sulfide Minerals of Copper-Nickel Ores. *Journal of Mining Science*. Vol. 39 (3), pp 281-286.

- [36] Liu, Z., & Doyle, F. M. Modeling Metal Ion Removal in Alkylsulfate Ion Flotation Systems. *Minerals and Metallurgical Processing*, Vol. 18 (3), 167-171, (2001).
- [37] Shigehito D., Akinobu H., Bienvenu B.A., and Mizuhata M. (2009). α - Ni(OH)₂ Films Fabricated by Liquid Phase Deposition Method. *Thin Solids Films*, Vol. 517 (5), pp 1546-1554.
- [38] Guo-riu F., Zhong-ai H., Li-jing X., Xiao-qing J., Yu-long X., Yao-xian W., Zi-yu Z., Yu-ying Y., and Hong-ying W. (2009). Electrodeposition of Nickel Hydroxide films on Nickel Foil and its Electrochemical Performances for Supercapacitor. *International Journal of Electrochemical Science*. Vol. 4, pp 1052-1062.
- [39] Atkins, Peter. Jones, Loretta. "Principios de Química: los caminos del descubrimiento". 3ra edición, 1ra reimpresión 2006, Ed. Médica-Panamericana. B.A. Arg. pp 17.
- [40] Marta S.M., and Francisca S.C., (2000). The Chemical Composition of "Multimistura" as a Food Supplement. *Food Chemistry*. Vol. 68, No. 1, pp 41-44.
- [41] www.biologia.edu.ar